ARSENIC MOBILIZATION THROUGH BIOREDUCTION OF IRON OXIDE NANOPARTICLES

by

Jonathan W. Roller

A thesis submitted in partial fulfillment of the requirements for the degree of

Master of Science
(Geosciences)

Dr. Madeline Schreiber (Co-Advisor)
Dr. Christopher Tadanier (Co-Advisor)
Dr. Donald Rimstidt

August 12, 2004

Virginia Polytechnic Institute and State University
Blacksburg, Virginia

Keywords: arsenic, Fe(III) reduction, *Geobacter metallireducens*

Arsenic Mobilization Through Bioreduction of Iron Oxide Nanoparticles

Jonathan W. Roller

Abstract

Arsenic sorbs strongly to the surfaces of Fe(III) (hydr)oxides. Under aerobic conditions, oxygen acts as the terminal electron acceptor in microbial respiration and Fe(III) (hydr)oxides are highly insoluble, thus arsenic remains associated with Fe(III) (hydr)oxide phases. However, under anaerobic conditions Fe(III)-reducing microorganisms can couple the reduction of solid phase Fe(III) (hydr)oxides with the oxidation of organic carbon. When ferric iron is reduced to ferrous iron, arsenic is mobilized into groundwater. Although this process has been documented in a variety of pristine and contaminated environments, minimal information exists on the mechanisms causing this arsenic mobilization.

Arsenic mobilization was studied by conducting controlled microcosm experiments containing an arsenic-bearing ferrihydrite and an Fe(III)-reducing microorganism, *Geobacter metallireducens*. Results show that arsenic mobility is strongly controlled by microbially-mediated disaggregation of arsenic-bearing iron nanoparticles. The most likely controlling mechanism of this disaggregation of iron oxide nanoparticles is a change in mineral phase from ferrihydrite to magnetite, a mixed Fe(III) and Fe(II) mineral, due to the microbially-mediated reduction of Fe(III). Although arsenic remained associated with the iron oxide nanoparticles and was not released as a hydrated oxyanion, the arsenic-bearing nanoparticles could be readily mobilized in aquifers. These results have significant implications for understanding

arsenic behavior in aquifers with Fe(III) reducing conditions, and may aid in improving remediation of arsenic-contaminated waters.

Table of Contents

Abstract ii

Table of Contents iv

1. Introduction 1

    Arsenic in nature 1

    Arsenic form and speciation 2

    Arsenic toxicity 2

    Arsenic adsorption 3

    Microbial impacts on arsenic mobility 5

2. Methods and Materials 9

    Experimental plan 9

    Preparation and characterization of 2 line ferrihydrite (2LFH) 10

    Arsenic adsorption onto ferrihydrite 11

    Sorptive capacity of ferrihydrite 13

    Culturing *Geobacter metallireducens* 14

    Microcosm preparation 16

    Microcosm sampling 16

    Analytical methods 18

        Arsenic 18

        Fe(II)/Fe_T 18

        Other dissolved analytes 19

        Hydrogen 19

3. Results and Discussion 20

    Growth of *Geobacter metallireducens* 20

    Reduction of ferrihydrite by *Geobacter metallireducens* 25

    Phase distribution of iron 26

    Arsenic mobilization 29

    Phase distribution of arsenic 31

    Mechanisms of arsenic mobilization 32

4. Implications 34

5. Conclusion 34

6. References 36
7. Appendices 41

List of Figures

Figure 1
Conceptual models of arsenic mobilization through Fe(III)-reduction coupled with organic carbon oxidation 8
Figure 2
TEM diffraction pattern of 2LFH synthesized 11
Figure 3
Arsenate sorption isotherms for ferrihydrite in the presence of 0.01M NaCl and minimal mineral salts media 13
Figure 4
Arsenate adsorbed vs. initial arsenic in solution for ferrihydrite in 0.01M NaCl and in media 14
Figure 5
Geobacter metallireducens pictures 20
Figure 6
Growth curve of GS-15 on ferric citrate media 21
Figure 7
Color change due to ferric citrate reduction by GS-15 21
Figure 8
Fe(II) in slurry samples produced after inoculation of GS-15 in iron gel media 22
Figure 9
Color change due to Iron gel reduction by GS-15 23
Figure 10
Relative hydrogen peak areas of biotic and abiotic ferric citrate and iron gel medias after 1 and 9 weeks 24

Figure 11
Fe(II) in microcosm slurry produced over time for the four different types of microcosms 26
Figure 12
Fe_T [Fe(II)+Fe(III)] present in filtered (0.2 micron), unfiltered, and filtered/ultracentrifuged samples 28
Figure 13
Total Fe and Fe(II) in the filtered and filtered/ ultracentrifuged samples on day 20 29
Figure 14
Arsenic in filtered and filtered/ultracentrifuged samples 30
Figure 15
Ratio of iron and arsenic that passed through a 0.2 micron filter to the total iron (0.056 M) and arsenic (50 or 100 μM) in the media 32

List of Appendices

Appendix A
Ferrihydrite (iron gel) synthesis 41
Appendix B
Procedure for loading iron gel media with arsenic 42
Appendix C
Sorption isotherm data for arsenate on ferrihydrite in the presence of 0.01 M NaCl and in the presence of media 43
Appendix D
Anaerobic water procedure 45
Appendix E
Deoxygenated ultrapure nitrogen sparging method 46
Appendix F
Resazurin: oxygen indicator procedure 47

Appendix G

Geobacter metallireducens media recipe 48

Appendix H

Ferrozine method 50

Appendix I

Fe(II) data for biotic ferric citrate media 51

Appendix J

Fe(II) data for growth curves in biotic and abiotic iron gel medias 52

Appendix K

Relative peak areas of hydrogen in biotic and abiotic trials of ferric citrate and iron gel media 1 week and 9 weeks after inoculation 53

Appendix L

Total Fe(II) produced data in microcosm slurry 54

Appendix M

Total Fe data in filtered, unfiltered, and filtered/ ultracentrifuged samples 56

Appendix N

Total Fe (Fe(II) + Fe(III)) and Fe(II) data in filtered and filtered/ultracentrifuged samples on day 20 59

Appendix O

Arsenic data in filtered and filtered/ultracentrifuged samples 60

Appendix P

Fraction of total iron or arsenic that passed through the 0.2 micron membrane 62

Introduction

Arsenic in Nature

Of all the possible routes for arsenic exposure in the environment, drinking water containing elevated arsenic poses the greatest threat to human health (Smedley and Kinniburgh, 2002). In addition to causing cardiovascular and neurological diseases, arsenic exposure is also linked to skin, lung, bladder, and kidney cancer (NRC, 1999). In October 2001, the EPA announced that it would lower the arsenic maximum contaminant level (MCL) in drinking water from 50 μg/L to 10 μg/L. The effective date for this new standard is February 2006 (Smith et al., 2002).

Arsenic concentrations in natural waters can vary greatly, ranging from less than 0.5 μg/L to more than 5,000 μg/L (Smedley and Kinniburgh, 2002). Although elevated arsenic in groundwater can be found in a variety of hydrogeologic regions, it occurs most commonly in geothermal regions (Moore et al., 1988; Langner et al., 2001; Welch et al., 1988), areas of evaporative concentration (e.g., Welch et al., 1988), alluvial and deltaic aquifers containing iron oxides (Holm et al., 1979; Islam et al., 2004; Nickson et al., 2000; Ahmed et al., 2004; Zheng et al., 2004; Akai et al., 2004), and areas that contain arsenic-bearing sulfide deposits (Schreiber et al., 2000). Sources of arsenic to natural waters include naturally-occurring minerals, such as arsenopyrite, arsenian pyrite, orpiment, and realgar, as well as anthropogenic sources such as agricultural applications, wood preservation, and glass production (Welch et al., 2000).

The speciation and phase distribution of arsenic in the environment is complex because it is influenced by adsorption, oxidation-reduction, and precipitation-dissolution, as well as microbially-mediated reactions. Collectively, these processes determine the

form (inorganic vs. organic), the speciation (arsenite As(III) vs. arsenate As(V)), and the mobility of arsenic in natural waters.

Arsenic form and speciation

Arsenic occurs in the environment in four oxidation states: As(-III), As(0), As(III), and As(V) (Oremland and Stolz, 2003). The most common species of arsenic found in natural waters are the inorganic oxyanions, trivalent arsenite (H_3AsO_3, $H_2AsO_3^-$, $HAsO_3^{2-}$) and pentavalent arsenate ($H_2AsO_4^-$, $HAsO_4^{2-}$ and H_3AsO_4). In addition, there are a variety of organic forms of arsenic such as methanearsonic acid and dimethylarsenic acid (Andreae, 1986). As(III) is the more toxic form of the species (Andreae, 1986; Winship,1984). The main abiotic factors that control the speciation of arsenic are redox potential (Eh) and pH (Smedley and Kinniburgh, 2002). Under oxidizing conditions, arsenate is the primary arsenic species present in natural waters, whereas under reducing conditions, arsenite species predominate. However, the relative distribution of As(III) and As(V) is often far from thermodynamic equilibrium, likely due to microbial activity, sorption processes, the presence of strong oxidants and reductants, and relatively slow kinetics of abiotic oxidation (Eary and Schramke, 1990) and reduction (Peterson and Carpenter, 1986).

Arsenic toxicity

Arsenic is both a toxin and a carcinogen. Toxic effects of ingesting arsenic include cardiovascular, pulmonary, immunological, neurological, and endocrine disease (EPA, 2001). The varying toxicity of arsenic species is related to differences in

molecular structure. Of the two most common arsenic species in groundwater, arsenite is the more toxic species because it readily attaches to thiol groups present in many enzyme active centers, resulting in an especially broad inhibitory activity (Knowles and Benson, 1983). Conversely, organoarsenicals are relatively harmless because they are generally not metabolically converted to the more toxic inorganic species during passage through animal systems (Andreae, 1986).

Arsenic-induced cancer is thought to result from changes in cellular redox control mediated by altered glutathione (GSH) levels (Chouchane and Snow, 2001). Glutathione, a small protein and powerful antioxidant, can potentially bind toxins such as heavy metals, solvents, and pesticides, and transform them into forms more readily excreted in urine or bile. Preliminary research has shown that glutathione is associated with protection against some forms of cancer (Sen, 1997). However, glutathione supplements cannot be efficiently absorbed in humans (Witschi et al., 1992). For this reason glutathione cannot be readily replenished, and when arsenic binds with glutathione in humans, the potential for cancer increases.

Arsenic Adsorption

Arsenic readily adsorbs to several types of minerals commonly found in aquifers including hydrous oxides of iron, aluminum, and manganese, and clay minerals (Stollenwerk, 2003). Of these minerals the most efficient arsenic adsorbents are Fe(III)-(hydr)oxides, including ferrihydrite (a poorly crystalline Fe(III) (hydr)oxide), goethite, hematite, and magnetite (Pierce and Moore, 1980; Fuller et al., 1993; Raven et al., 1998; Stollenwerk, 2003).

Besides the mineral type, the primary factors that influence arsenic sorption are speciation, pH, and the presence of competing anions (Chiu and Hering, 2000; Fuller et al., 1993; Pierce and Moore, 1980; Raven et al., 1998; Wilkie and Hering, 1996; Barrow, 1974; Davis et al., 2001; Manning and Goldberg, 1996; Roy et al., 1986). Although it has been assumed that As(V) adsorbs to minerals more strongly than As(III), recent studies have shown that the relative affinities of Fe(III)-(hydr)oxides for As(III) and As(V) depends on solution composition and surface characteristics, and that As(III) may actually adsorb more strongly to hydrous ferric oxides and goethite than As(V) in the circumneutral pH range (Dixit and Hering, 2003). Arsenic adsorption is highly pH dependent because dissociation of its weakly acidic oxyanion forms results in neutrally to negatively charged species at pH values of natural waters. Arsenite exists predominantly as $H_3AsO_3^0$ and $H_2AsO_3^-$ with $pK_{a,1}$ and $pK_{a,2}$ values of 9.2 and 12.7 (Goldberg, 2002), exhibiting maximum adsorption to (hydr)oxide minerals at neutral pH (Pierce and Moore, 1980). The acidic properties of arsenate are very similar to those of orthophosphate, with $pK_{a,1}$, $pK_{a,2}$, and $pK_{a,3}$ values of 2.3, 6.8, and 11.6 respectively. Thus, arsenate is generally present in natural waters as $H_2AsO_4^-$ and $HAsO_4^{2-}$ and is most effectively adsorbed to minerals at low pH (Dzombak and Morel, 1990; McBride, 1994).

Another factor that impacts the adsorption of arsenic to minerals is the presence of competitive anions, such as phosphate, sulfate, carbonate, and silicate; that have similar physico-chemical characteristics that are similar to arsenate. Adsorption of oxyanions is dependent on the "shared charge", defined as the ratio of the valence of the central atom to the number of bonded oxygen atoms, and the electronegativity of the oxyanion (McBride, 1994). However, if these competitive anions are introduced after

arsenate has already been adsorbed, there is very little desorption of arsenate (Pierce and Moore, 1980).

Microbial Impacts on Arsenic Mobility

In addition to geochemical controls such as speciation and surface adsorption, microbial activity can also directly impact arsenic mobility in soils and natural waters (Cullen and Reimer, 1989). Microbial species are capable of reducing As(V) to As(III) (Ahmann et al., 1994; Andreae, 1983; Langner and Inskeep, 2000; Laverman et al., 1995; Newman et al., 1997; Zobrist et al., 2000) and also capable of oxidizing As(III) to As(V) (Gihring et al., 2001; Langner et al., 2001; Wilkie and Hering, 1998).

Microbial activity can also indirectly affect arsenic partitioning. Dissimilatory iron reduction, in which bacteria gain energy by coupling reduction of Fe(III) to Fe(II) with oxidation of an electron donor such as organic carbon or H_2, is a common respiration pathway in aquifer systems. Several Fe-(hydr)oxides are readily reduced microbially, including ferrihydrite, goethite, and hematite (Lovley, 2000). Common Fe(III) respiring microorganisms include *Geobacter metallireducens*, *Geobacter sulfurreducens*, *Geothrix fermentans, Geovibrio ferrireducens,* and *Shewanella, Ferrimonas,* and *Aeromonas* species (Lovley, 2000). Under anaerobic conditions, as these bacteria reduce solid forms of Fe(III) to more soluble Fe(II), adsorbed trace elements and nutrients such as arsenic may be mobilized in groundwater.

Previous studies have documented the occurrence of elevated groundwater arsenic concentrations in aquifers containing arsenic-bearing iron oxides (Zobrist et al., 2000; Ahmann et al., 1997; Islam et al., 2004; Nickson et al., 1998; Stüben et al., 2003).

Mobilization of arsenic due to the microbial reduction of As(V) to As(III) on iron oxides was investigated by Zobrist et al. (2000), Ahmann et al. (1997), and Islam et al. (2004). Zobrist et al. (2000) showed that the species *Sulfurospirillum barnesii* can reduce As(V) adsorbed to ferrihydrite and aluminum hydroxides to As(III). Although the organism was shown to reduce ferrihydrite, the authors attributed the bulk of arsenic mobilization directly to arsenate reduction. Microbially-mediated reduction of As(V) to As(III) was also observed by Islam et al. (2004) in sediment collected from the Bengal delta. The authors suggested that arsenic mobilization from sediment into water was controlled by the microbial respiration of As(V) to As(III).

In a study with *Shewanella alga* strain BrY and the mineral scorodite ($FeAsO_4 \cdot 2H_2O$) (Cummings et al., 1999), it was shown that As(V) was mobilized in water as a result of dissimilatory reduction of Fe(III) in scorodite to Fe(II) without reduction of As(V) to As(III). However, because the study did not specifically distinguish between As(V) from coordinated positions within the mineral and As(V) that was sorbed onto the surface of the mineral, the true mobilization mechanism is unclear.

As illustrated in the studies described above, microorganisms can potentially mediate mobilization of arsenic from Fe-(hydr)oxides, whether adsorbed on or contained within the mineral structure, by several distinctly different mechanisms. However, understanding of the fundamental biochemical and physicochemical processes involved in these arsenic mobilization mechanisms is still limited, and has been complicated by the often contradictory and interchangeable terminology used in the literature to describe them. As defined here and used throughout this work, the term *mobilization* will be used as a general term to describe arsenic partitioning from solid to solution phase, regardless

of its form. *Release* refers to processes that mobilize hydrated arsenic oxyanions directly from the mineral phase into solution, whereas *disaggregation* refers to processes that mobilize arsenic associated with a suspended mineral-phase nanoparticle that can be transported in natural waters. Release could potentially be caused by competitive adsorption of surface active metabolites, or through reduced affinity of arsenic for the surface due to Fe (III) reduction at the surface or direct reduction of sorbed arsenic (Figure 1b). Disaggregation may be due to the freeing of As-Fe-mineral clusters through reductive dissolution of the underlying Fe(III)-(hydr)oxide, or dispersion of arsenic bearing nanoparticles that form larger colloidal aggregates (Figure 1c). Because arsenic contamination of natural waters due to mobilization from mineral surfaces is a significant route of human arsenic exposure worldwide, improved understanding of the biologically-mediated mechanisms that partition arsenic between solid and solution phases is required for development of effective treatment and remediation strategies.

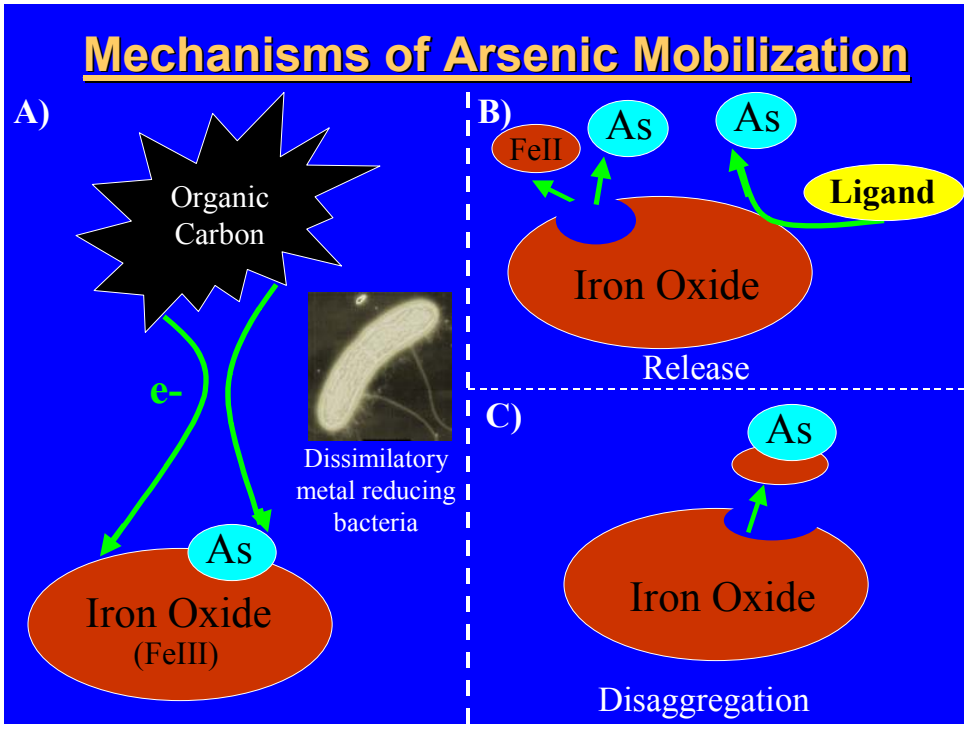

Figure 1: Conceptual models of arsenic mobilization through Fe(III)-reduction coupled with organic carbon oxidation: a) transfer of electrons from organic carbon to iron or arsenic via a dissimilatory metal reducing microorganism, b) arsenic release by competitive desorption or reduced affinity for surface after iron reduction, and c) disaggregation of arsenic-bearing nanoparticles

The objective of this study was to evaluate the mechanisms and quantify the kinetics of arsenic mobilization associated with microbial respiration on ferric-iron minerals. A series of microcosm experiments was conducted using *Geobacter metallireducens* (sp. GS-15) with ferrihydrite as the sole terminal electron acceptor, to which As(V) was previously adsorbed. GS-15 was chosen because it is relatively abundant in nature, is capable of oxidizing a wide range of organic carbon sources, including anthropogenic compounds such as toluene, but is unable to directly reduce arsenate to arsenite (Ahmann et al., 1997). Ferrihydrite was chosen as the Fe(III)

mineral source because it has high surface area and is bioavailable to GS-15 (Pierce and Moore, 1980; Fuller et al., 1993; Raven et al., 1998; Stollenwerk, 2003).

Methods and Materials

Experimental Plan

Anaerobic microcosms were used to evaluate the mechanisms and kinetics of arsenic mobilization due to microbially mediated reduction of ferrihydrite. Prior to introduction into the microcosms, As(V) was sorbed onto ferrihydrite iron gel at pH 7 in a pH-stat system. *G. metallireducens* GS-15, cultured in a ferric citrate media, was used as the inoculant for biotic controls, with acetate as the carbon source/electron donor. Because all microcosms were prepared and maintained in an environmental chamber with 95% N_2 and 5% H_2 atmosphere, hydrogen was also available as an electron donor. Abiotic controls were also prepared by inoculating ferrihydrite media with heat-killed cells or sterile ferric citrate media.

Four sets of microcosm trials were conducted to determine rates of Fe(III) reduction and arsenic mobilization from ferrihydrite iron gel in the presence and absence of GS-15. The first two trials were designed to examine the impact of varying arsenate concentrations loaded on iron gel (50 and 100 μM) on the corresponding rates of arsenic mobilization in the presence of GS-15. The third trial, which contained GS-15 and iron gel media without arsenate, was conducted to determine if the presence of arsenate inhibits or enhances microbially-mediated Fe(III) reduction. The last trial was an abiotic control, which contained iron gel media loaded with 100 μM arsenate inoculated with sterile ferric citrate media. All trials were conducted simultaneously with the same initial iron gel media. Each trial was conducted in triplicate.

Preparation and characterization of 2 line ferrihydrite (2LFH)

2-line ferrihydrite (2LFH) was chosen for this study because it typically has high surface area and is considered the most reactive of the iron minerals (Raven et al., 1998; Fuller et al., 1993). The 2LFH was synthesized using the method of Schwertmann and Cornell (Schwertmann and Cornell, 1991) modified by Glasauer et al. (2002) (Appendix A). A ferric chloride solution was brought to pH 7 by dropwise addition of 10N sodium hydroxide. The precipitate was centrifuged and rinsed several times to remove excess salts. Finally, the desalted precipitate was diluted to 1M Fe using milli-Q water.

Ferrihydrite can readily transform into more crystalline Fe-solids, such as goethite. This transformation depends on temperature, pH, and the presence of other solutes (Cornell and Schwertmann, 1996; Greffie et al., 2001), and appears to be dramatically accelerated by dehydration during freeze-drying. Therefore, a fresh batch of 2LFH was synthesized for each experiment and used in its hydrated state immediately after desalting to maintain a high surface area and minimize transformation to goethite.

The crystal structure and morphology of the 2LFH product was evaluated using diffraction patterns collected by transmission electron microscopy (TEM) (Janney et al., 2000). The d-spacings of the synthesized product were consistent with the known d-spacings of 2LFH (Figure 2). TEM analysis showed that the synthesized 2LFH consisted of 2-5 nm individual grains that were aggregated in 5 μm clumps. The tendency for 2LFH nanoparticles to aggregate into large clumps has also been observed by others (e.g. Greffie et al., 2001).

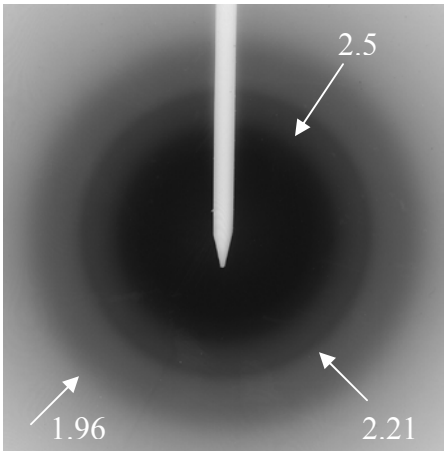

Figure 2: TEM diffraction pattern of 2LFH synthesized. Known d-spacings of 2LFH indicated.

The specific surface area was estimated to be 245 m^2/g using a combination of methods including N_2 BET analysis on freeze dried samples and geometric analysis using particle size distributions from TEM images and photon correlation spectroscopy performed using a Malvern ZetaSizer 3000HS instrument.

Arsenic adsorption onto ferrihydrite

Arsenic loaded Fe gel was prepared by diluting an aliquot of desalted 1 M gel with 0.01 M NaCl to a final Fe concentration of 0.056 M, and vigorously mixing the suspension for 2 hours under continuous sparging with ultrapure nitrogen to minimize CO_2 (Appendix B). A known concentration of As(V) was then added from a 1 M sodium arsenate stock solution, and the Fe-gel was allowed to equilibrate for 2 h. During equilibration of arsenate with the Fe-gel pH 7 was maintained using a Brinkmann Titrino Model 719 S pH stat and 0.1 N HCl titrant, and continuous sparging with CO_2-free ultrapure N_2 applied.

Because the intent of this study was to examine the microbially mediated mobilization of arsenic sorbed on ferrihydrite, sorption isotherms were prepared at pH 7 to determine the range of arsenic concentrations that would result in greater than 99 % of added arsenic initially sorbed onto the Fe-gel, both in the presence and absence of competing ligands such as phosphate and acetate contained in bacterial nutrient media. Aliquots of 1 M sodium arsenate stock solution were serially added to 400 mL of microcosm iron gel suspensions prepared either in 0.01 M NaCl or minimal mineral salts media (see below), with 2 h equilibration between additions. Samples for arsenic analysis were collected from the slurries at each arsenate concentration, filtered through a 0.2 micron membrane, and preserved with 10 μL of 2 N HCl. Sorbed As(V) was calculated by difference between each known total concentration and the residual concentration in each corresponding filtered sample. Arsenate sorption data were divided by ferrihydrite suspension density and specific surface area to produce sorption isotherms, as shown in Figure 3.

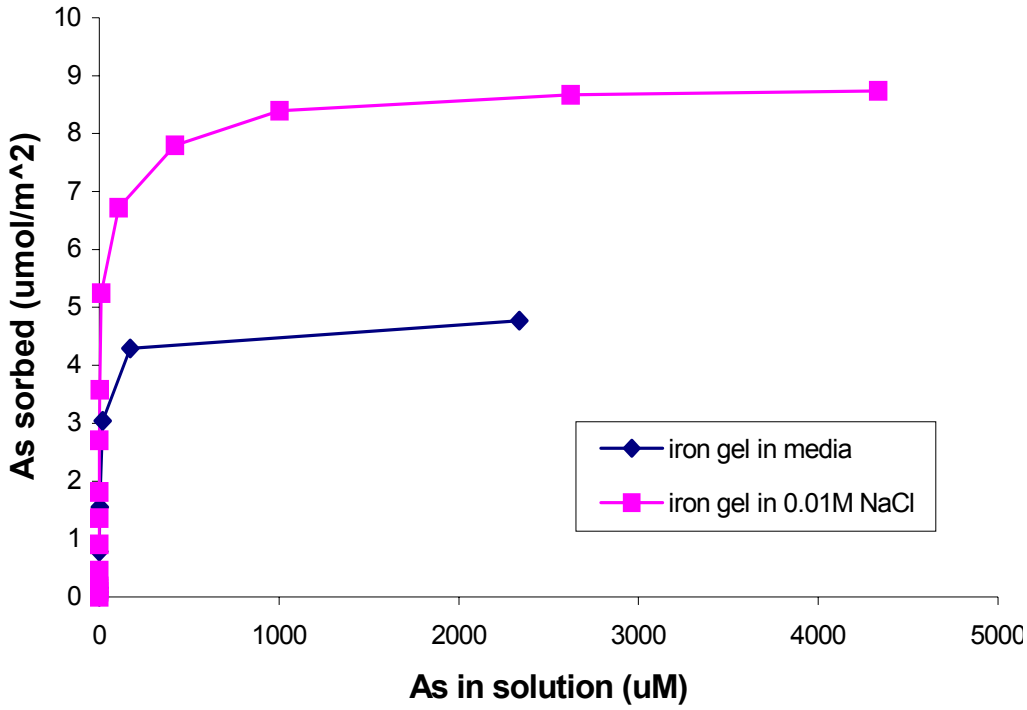

Figure 3: Arsenate sorption isotherms for ferrihydrite in the presence of 0.01 M NaCl and minimal mineral salts media.

Sorptive capacity of ferrihydrite

The arsenate isotherm experiments, prepared using iron gel and solutions of 0.01 M NaCl or minimum mineral salts media, with an ionic strength of ~0.12 M (Figure 3; Appendix C), show that the presence of competing anions in the media (i.e., phosphate and acetate) decreases the sorptive capacity of the iron gel. The concentration at which the iron gel surface is saturated can be more easily visualized by plotting the concentration of adsorbed arsenate vs. the initial solution arsenate concentration (Figure 4).

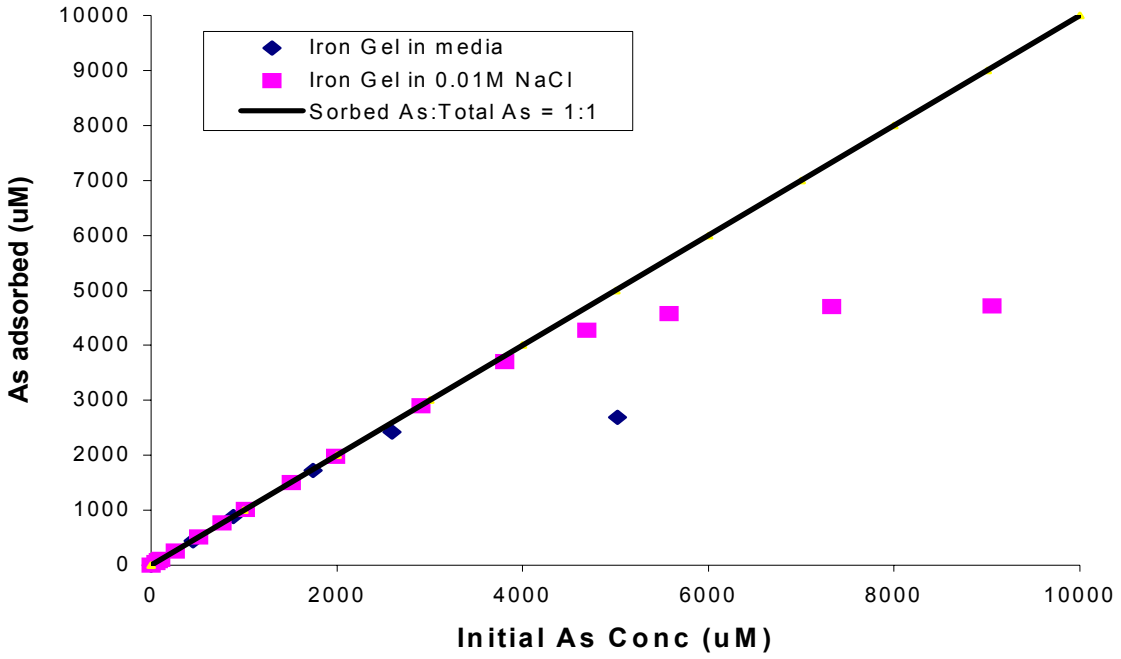

Figure 4: Arsenate adsorbed vs. initial arsenic in solution for ferrihydrite in 0.01M NaCl and in media. 45-degree trend line shows concentration at which the surface becomes saturated, releasing arsenic to solution.

The sorptive capacities of iron gel in 0.01 M NaCl and in nutrient media were fully exhasuted at arsenate concentrations greater than or equal to approximately 3500 μM and 1800 μM, respectively. These data were used to determine loading rates for arsenate on iron gel in GS-15 microcosm experiments. Arsenate concentrations of 50 and 100 μM were chosen because at these concentrations >> 99 % of arsenic was adsorbed.

Culturing Geobacter metallireducens

Because *G. metallireducens* is an obligate anaerobe, special precautions were taken to ensure that nutrient media was anaerobic prior to inoculation (Appendix D). Anaerobic water for media was prepared by first boiling nanopure deionized water for 20

minutes. Next, the water was bubbled with deoxygenated ultrapure nitrogen (Appendix E) for 45 minutes to encourage gas exchange. After sparging, the nanopure water was autoclaved for 45 minutes at 127^{o}C. The headspace of the bottle was then replaced with deoxygenated ultrapure nitrogen. Finally, the bottle was placed in an environmental chamber (95% N_2, 5% H_2) and allowed to equilibrate with the chamber atmosphere for 24 h by loosening the cap and mixing the bottle on a shaking table. The success of removing oxygen from the water was verified by measuring the dissolved oxygen (DO) content of the water colorimetrically using resazurin (Appendix F) and the dissolved oxygen CHEMets® Kit K-7540; the resulting DO of the water was <1 ppb O_2.

G. metallireducens GS-15 was grown using a minimal salts media, #1768 broth, recommended by the American Type Culture Collection (ATCC) (Appendix G). After preparing anaerobic water, 1 L of media was made by adding the following ACS grade chemicals: 2.5 g $NaHCO_3$, 0.25 g NH_4Cl, 0.6 g $NaH_2PO_4 \cdot H_2O$, 0.1 g KCl, and 6.8 g sodium acetate. Next, 10 mL/L each of filter sterilized Wolfe's vitamin solution and Wolfe's mineral solution (ATCC #53774) were added to the media and the pH adjusted to 7. Iron was added to the media either as ferric citrate or Fe-gel, with a total iron concentration of 0.056 M as Fe for both types of media. Finally, anaerobic media was equilibrated with a 95% N_2: 5% H_2 atmosphere for 24 h in an environmental chamber, and inoculated with live GS-15 cells (courtesy of Dr. Michael McCormick, Hamilton College, NY). Growth in subculture was verified by direct cell count using visible light and epifluorescent microscopy with Gram and acridine orange stains, respectively.

Microcosm preparation

Microcosms were prepared using arsenic-loaded iron gel, mineral salts media, and GS-15 as follows. Anaerobic Fe-As-gel media in 10 mL aliquots was pipetted into 15 mL serum vials, and allowed to equilibrate with a 95% N_2 : 5% H_2 atmosphere in an environmental chamber for 24 hours. Several microcosms were sacrificed prior to inoculation and the dissolved oxygen verified to be less than 1 ppb. For biotic trials, microcosms were inoculated with 0.83mL of GS-15 cultured for 20 days on ferric citrate as terminal electron acceptor. At this point in the *G. metallireducens* growth cycle, reduction of Fe(III) to Fe(II) was measurably complete, thus no ferric iron was added to the microcosms with the inoculum. For abiotic trials, microcosms were inoculated with either autoclaved inoculum or sterile ferric citrate media. Inoculated microcosms were capped with butyl rubber stoppers, crimp-sealed, and placed on a rotary shaker at 10 rpm. All microcosm experiments were conducted in triplicate.

Microcosm sampling

Samples were collected from each microcosm slurry (iron gel + media) once a day for 5 days and then every other day for approximately three weeks. Microcosms were vigorously shaken prior to each sampling event to maintain a constant solid to solution ratio during the experiment. The phase distribution of iron and arsenic in the microcosms was determined through filtration (0.2 micron) and ultracentrifugation (109,000 rcf for 1 h). Filtration removes colloidal and particulate iron (>200 nm), whereas nanoparticles (<200 nm) pass through the membrane. Ultracentrifugation settles out nanoparticles, leaving dissolved (hydrated oxyanion) species in the supernatant. By

measuring the iron and arsenic in the filtered and filtered/ultrcentrifuged samples, the phase distribution (colloid vs. nanoparticle vs. hydrated oxyanion) of iron and arsenic could be determined.

Two aliquots were collected from each microcosm at each sampling event: 0.75 mL of well-mixed slurry was filtered through a 0.2 micron membrane syringe filter, and 50 μL of slurry was diluted with 940 μL of milli-Q water and preserved with 10 μL of 2N HCl. Both filtered and unfiltered samples were analyzed for Fe(II) and total iron (Fe_T), and the filtered samples were analyzed for arsenic. Arsenic was measured directly on filtered samples by graphite furnace atomic adsorption spectroscopy (GFAAS) without further sample processing. Prior to iron analyses, samples were digested for 24 h by adding 1 mL of 0.5 N HCl to either the unfiltered samples or 50 μL of filtered sample diluted with 950 μL milli-Q water. Iron analyses were performed colorimetrically using the ferrozine method. The remaining portions of the filtered samples were then ultracentrifuged at 109,000 rcf for 1 h and the supernatant carefully removed by micropipette. Arsenic and iron analyses were performed on the ultracentrifuged supernatant as before. Digested samples were also analyzed for low molecular weight organic acids by ion exclusion chromatography. Finally, selected samples were preserved with EDTA and arsenic speciated by strong anion exchange to distinguish between As(V) and As(III).

Hydrogen was monitored in the headspace of separate sacrificial microcosms, which were prepared using 6 mL of media in a 10 mL serum vial and inoculated with 0.5 mL of 7 day-old biotic ferric citrate media; abiotic microcosms were inoculated with 0.5 mL of heat killed 7 day-old biotic ferric citrate media. The serum vials were then sealed

with a butyl rubber stopper and crimped with an aluminum seal. Headspace samples, collected by puncturing the butyl rubber stopper of an unopened serum vial with a needle and withdrawing 1 mL of headspace into a gas-tight syringe, were taken at 1 week and 9 weeks after inoculation.

Analytical Methods

a) Arsenic

Arsenic was measured on the filtered and filtered then ultracentrifuged samples using GFAAS (Varian Spectra 220Z) with a Zeeman background correction system. This method has a detection limit for arsenic of approximately 3 μg/L (0.04 μM). Samples were manually diluted in cases where arsenic concentration was higher than the calibration curve linear range (0 μg/L to 100 μg/L). Arsenic speciation (arsenite and arsenate) was conducted by strong anion exchange column (SAX) separation, followed by GFAAS analysis. The separation involves eluting a sample through a column wherein neutral species (arsenite) pass through the column while the negatively charged species (arsenate) are retained on the column and extracted separately with nitric acid (Le et al. 2000; Garbarino et al. 2002).

b) Fe(II)/Fe_T

Fe(II) and Fe_T were measured colorimetrically using the ferrozine method (Stookey, 1970) as modified by Lovley and Philips (1986) (Appendix H). Ferrozine solution was prepared by adding 1g of ferrozine to 1 L of 50mM HEPES buffer. Fe(II) was measured by adding 200 μL of unfiltered or 200 μL filtered or ultracentrifuged digest

to 1.5 mL of the ferrozine solution and measuring absorbance at 562 nm on a Beckman-Coulter DU 640 spectrophotometer after 15 min. 150 μL of 0.5 N hydroxylamine was then added to the ferrozine treated samples to reduce any Fe(III) to Fe(II), and Fe_T measured as absorbance at 562 nm following 5 min. incubation. Absorbance values for Fe(II) and Fe_T were converted to mg/L Fe through comparison to known Fe(II) standards.

c) Other dissolved analytes

Acetate and citrate from nutrient media, as well as any other low molecular weight organic acid metabolites, were measured in digested samples of unfiltered and filtered then ultracentrifuged samples by ion exclusion chromatography using a Dionex® DX 120 ion chromatograph with a Dionex® AS6 column. The eluent used was 0.4 mM heptafluorobutyric acid and the regenerant used was 5 mM tetrabutylammonium hydroxide.

d) Hydrogen

Hydrogen in microcosm headspace samples was analyzed by a Trace Analytical® gas chromatograph equipped with a reduced gas detector (RGD). Due to the high (up to 5%) concentration of H_2 in environmental chamber and the low (5 μM) maximum detection limit of the RGD, headspace samples were diluted by a factor of 5 with ultrapure nitrogen prior to injection. Because relative changes, and not absolute concentrations, of hydrogen were of interest in this study, calibration with external standards was not performed; results are presented as relative peak areas.

Results and Discussion

Growth of Geobacter metallireducens

In addition to verifying the presence of cells in microcosms by direct cell count using visible light and epifluorescent microscopy with Gram (Figure 5a) and acridine orange (Figure 5b) stains, respectively, growth of *Geobacter metallireducens* was evaluated by measuring Fe(II) production.

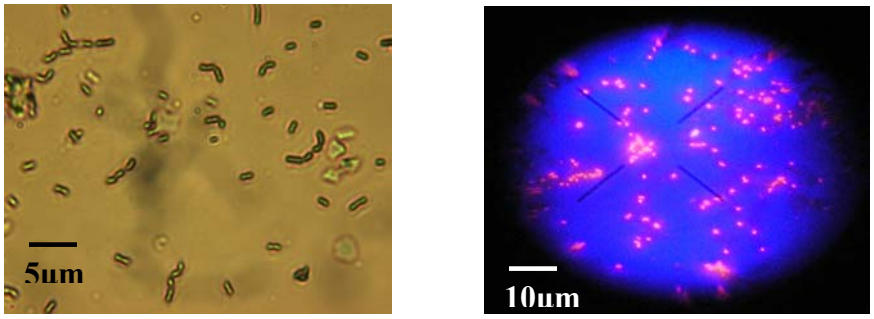

(a) (b)

Figure 5: *Geobacter metallireducens* a) dyed with Gram stain and observed using a light microscope and b) dyed with acridine orange stain and observed using an epifluorescent microscope.

GS-15 was first grown by injecting 6 mL of ferric citrate media with 0.5 mL of inoculant within a sealed and crimped 10 mL serum vial. Growth of GS-15 on ferric citrate media was confirmed through measurement of Fe(II) in samples filtered with a 0.2 micron membrane and preserved with 2N HCl taken every few hours (Figure 6; Appendix I). The lag phase of growth (0-2 d), characterized by a slight increase in Fe(II), is followed by a rapid Fe(II) increase (2-4.5 d), correlated with the growth phase. The decline of Fe(II) after day 4.5 represents the death phase, in which Fe(II) is likely removed from solution through adsorption to cells.

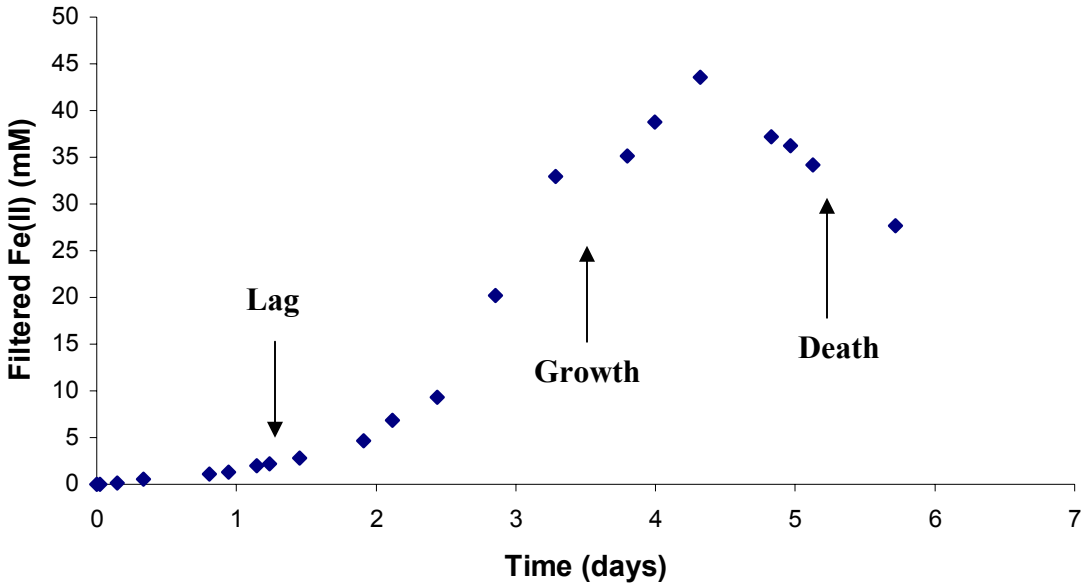

Figure 6: Growth curve of GS-15 on ferric citrate media.

Growth of GS-15 on ferric citrate correlates with a color change in the media, as the Fe(III) is progressively reduced (Figure 7). During the first 2 days (lag phase), the media turns from an orange color to a dark brown. From days 2 to 5, the media changes from dark brown to clear, indicating complete reduction of complexed Fe(III). At day 5, analysis of the media showed no difference in Fe_T and Fe(II) concentrations, indicating that all iron was present as Fe(II).

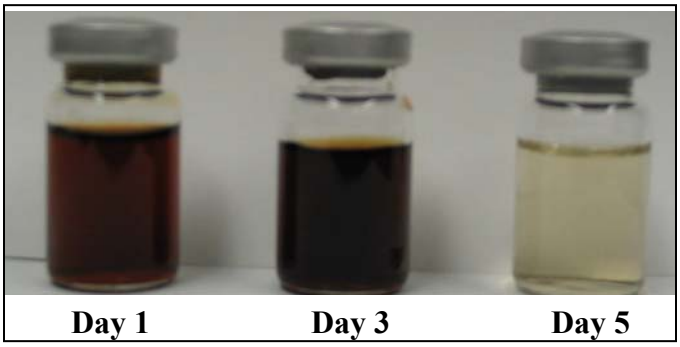

Figure 7: Ferric citrate reduction by GS-15 over time. Note color change from red to black to clear as Fe(III) is reduced to Fe(II).

Growth of GS-15 on solid phase Fe(III) was evaluated by inoculating iron gel with GS-15 grown on ferric citrate media for at least 5 days. Growth is indicated by the increases in Fe(II) in the slurry in biotic trials; the abiotic control shows no Fe(II) production (Figure 8; Appendix J).

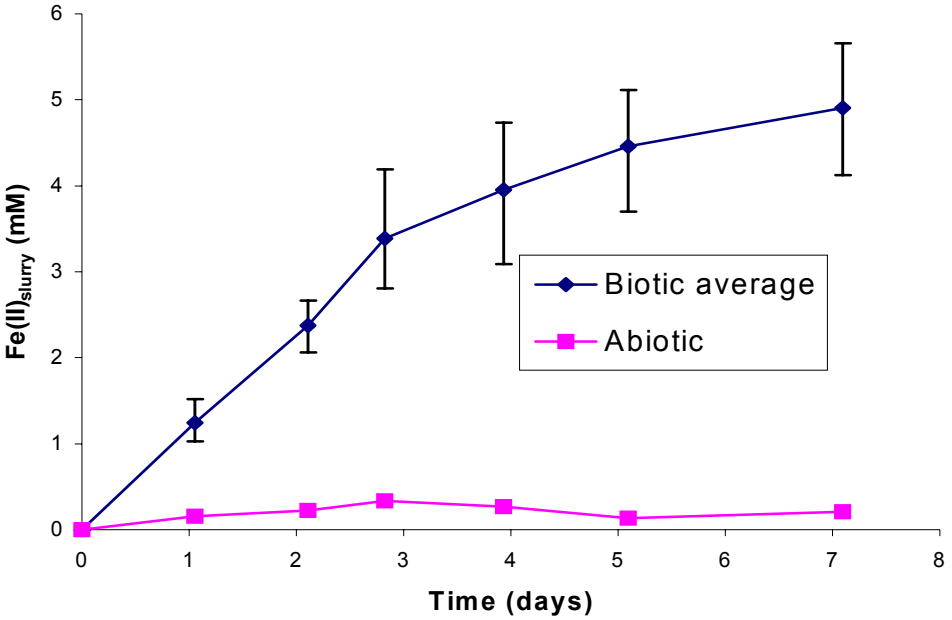

Figure 8: Fe(II) in slurry samples produced after inoculation of GS-15 in iron gel media. Biotic average represents an average of 6 replicate experiments. Error bars show the maximum and minimum Fe(II) concentrations of the 6 biotic trials.

Similar to the ferric citrate media, the iron gel media underwent a color change after inoculation. During the first 5 days, the biotic iron gel media changed from a reddish-brown color to a dark brown, almost black color (Figure 9), suggestive of the reduction of reddish-brown Fe(III) oxides to black mixed Fe(II)/Fe(III) minerals.

Figure 9: Iron gel reduction by GS-15. Reddish-brown color of iron gel apparent in Day 1; blacker color visible in Day 5.

The kinetics of Fe(III) reduction, as determined by Fe(II) production, was controlled by the Fe(III) source, as has been observed in other studies (e.g., Zobrist et al., 2000). The maximum rate of Fe(II) production in the ferric citrate media (Figure 6) occurs between days 2 and 4.5 and is approximately 17.3 mM/day, while in the iron gel, the maximum rate of Fe(II) production occurs between days 1 and 4 and is significantly lower, approximately 0.97 mM/day (Figure 8). Although the concentration of Fe(III) is the same for these two experiments (~0.056 M Fe), less Fe(III) is bioavailable in the iron gel media because iron within the mineral is inaccessible to the bacteria, while all of the Fe(III) in the ferric citrate media is in solution and is thus bioavailable. Additionally, some of the Fe(III) surface of the iron gel may be inaccessible to GS-15 because phosphate and other media constituents are absorbed to the surface sites.

Transformation of the 2LFH from an oxidized to a reduced state was examined using transmission electron microscopy (TEM). TEM diffraction patterns of abiotic and 2-day old biotic iron gel were consistent with known diffraction patterns of 2LFH. The

diffraction pattern of 5-day old biotic iron gel media was consistent with lepidocrosite [FeO(OH)]. Biotic iron gel that was 14 days old had a diffraction pattern consistent with the mixed Fe(II)/Fe(III) mineral, magnetite ($Fe^{2+}Fe_2^{3+}O_4$). Recent studies have shown that the microbial-mediated reduction of ferrihydrite to magnetite readily occurs (Kukkadapu et al., 2004). The presence of magnetite was further suggested in microcosms incubated for 60 d, in which many of the iron particles were attracted to a magnetic stir bar.

Microbial activity in the ferric citrate and iron gel media was further verified by comparing the relative concentrations of H_2 present in the headspaces of biotic and abiotic trials (Figure 10; Appendix K). Separate microcosms were prepared solely for hydrogen analysis to prevent gas exchange during media sampling. Headspace samples were taken from these sealed and crimped microcosms by puncturing the butyl rubber stopper with a syringe. Because hydrogen can be used by GS-15 as an electron donor (Lovley and Goodwin, 1988), decreases in hydrogen suggest microbial activity.

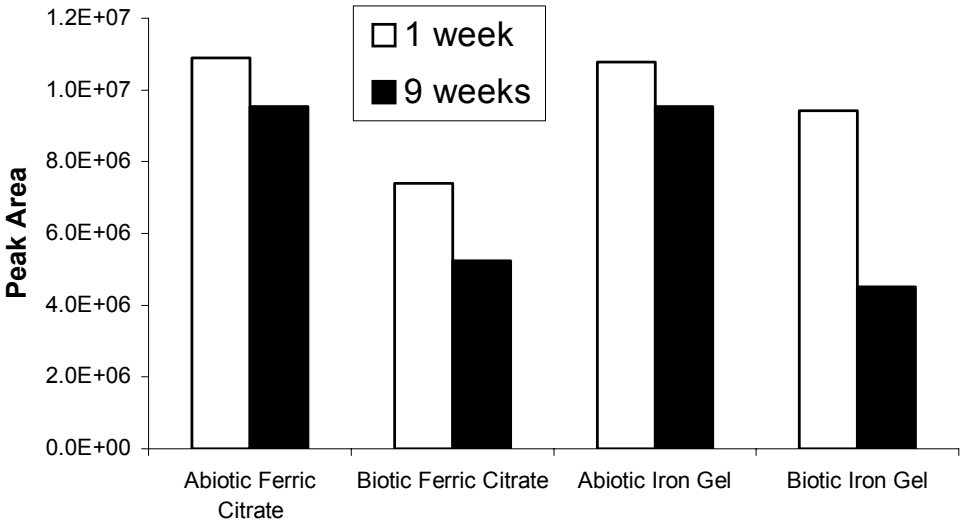

Figure 10: Relative hydrogen peak areas of biotic and abiotic ferric citrate and iron gel medias after 1 and 9 weeks.

Hydrogen concentrations in the abiotic trials decreased slightly from 1 to 9 weeks, while concentrations in the biotic trials were significantly lower, suggesting depletion of H_2 by GS-15 over the experimental period. Another interesting observation is that the iron gel media only has a slight decrease in H_2 concentration after the first week (assuming that abiotic control hydrogen represents time zero), while the ferric citrate media has a much more substantial drop in H_2 concentration during the same time period. This may be due to the faster acclimation of GS-15 cells to ferric citrate as a Fe(III) source than iron gel, leading to the GS-15 cells having a more rapid metabolism using ferric citrate. By week 9, however, the H_2 concentration in the biotic iron gel media decreased substantially, suggesting that the cells were actively depleting hydrogen. The slight decrease in H_2 concentration in the abiotic control between weeks 1 and 9 is likely due to loss in headspace when the butyl rubber stopper is punctured during sampling.

Reduction of Ferrihydrite by Geobacter metallireducens

Results of the analysis of Fe(II) in the slurry samples from the four trials are shown in Figure 11 (Appendix L). Over time, the Fe(II) produced in all three biotic trials steadily increased before reaching a plateau at about day 10, while the abiotic trial remained essentially flat throughout the monitoring period. These results indicate that Fe(III) reduction is actively occurring in the biotic trials and that abiotic (chemical) reduction is not a significant pathway for Fe(III) reduction in these experiments.

Although the differences in Fe(II) production between the three biotic trials are not statistically significant, an interesting observation is that the microcosms with the

higher concentration of arsenic loading (100 μM) had consistently higher Fe(II) production than trials with lower or no arsenic. One possible explanation for this is that a nutrient such as phosphate from the media is competitively desorbed by arsenate, making it more accessible to GS-15, thus allowing more Fe(III) reduction.

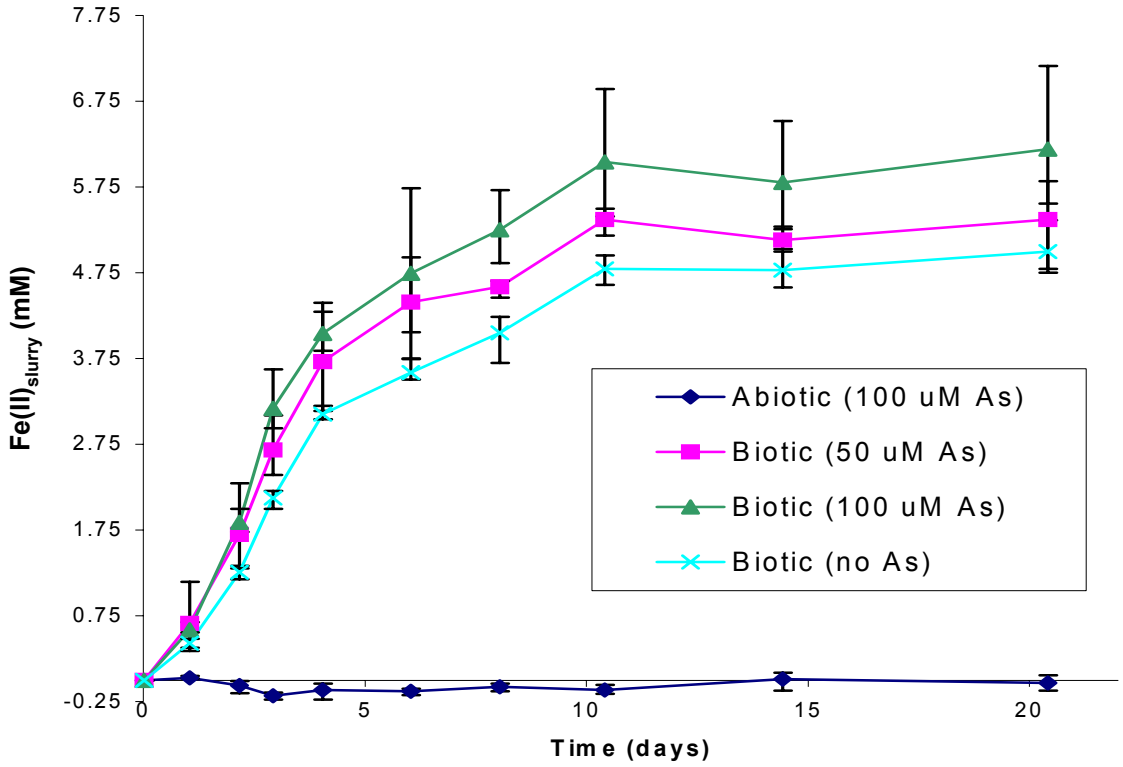

Figure 11: Fe(II) in microcosm slurry produced over time for the four different types of microcosms. Results are shown as averages of triplicates; error bars denote the maximum and minimum concentrations of Fe(II) for each triplicate.

Phase Distribution of Iron

An important observation made during these trials was that as time progressed the filtered samples from biotic trials became darker, while the filtered samples from abiotic trials remained clear. This phenomenon suggests that iron gel particles were passing

through the 0.2 micron membrane in biotic trials. Even when the samples were filtered using a 0.1 micron membrane, they still retained their dark brown color. It should be noted that when freshly prepared iron gel was filtered with a 0.2 micron membrane, the filtered solution was clear and analysis on the filtered solution showed no iron breakthrough.

Although the iron passing through the 0.2 micron membrane could have been soluble, the thermodynamics of the system do not support this hypothesis. The media contains approximately 0.03 M bicarbonate and at a pH of 7, the amount of Fe(II) that is produced is approximately 10 times larger than the solubility limit of siderite ($FeCO_3$). Another potential explanation for the passage of iron through the filter is that the iron was being organically complexed by organics produced by microbial activity. This theory was tested by analyzing samples for common microbially-produced low molecular weight organic acids. Besides acetate, which was added as an electron donor, and citrate, which was added through inoculation, analyses showed no other low molecular weight organic acids were being produced in the microcosms. Thus, it is unlikely that the iron passing through the 0.2 micron membrane was complexed by organic molecules produced by GS-15. The last explanation for the passage of iron through the 0.2 micron membrane is that the initially aggregated ferrihydrite nanoparticles were becoming disaggregated due to microbial activity.

To test the hypothesis that the ferrihydrite was being disaggregated, aliquots of the filtered microcosm samples were ultracentrifuged (109,000 rcf for 1 h) and analyzed for Fe_T (Appendix M). The Fe_T in unfiltered slurry samples remained constant at approximately 59 mM (Figure 12), indicating no change in microcosm solid: solution

ratios over time. In filtered samples Fe_T increased with time in biotic trials, but was essentially constant at 2.2 mM in abiotic trials. By comparison, Fe_T in all filtered/ultracentrifuged samples was quite low. These results indicate that 1) iron particles did pass through the 0.2 micron filter, 2) more particles passed through as the experiment progressed, and 3) the breakthrough of iron particles was related to microbial activity.

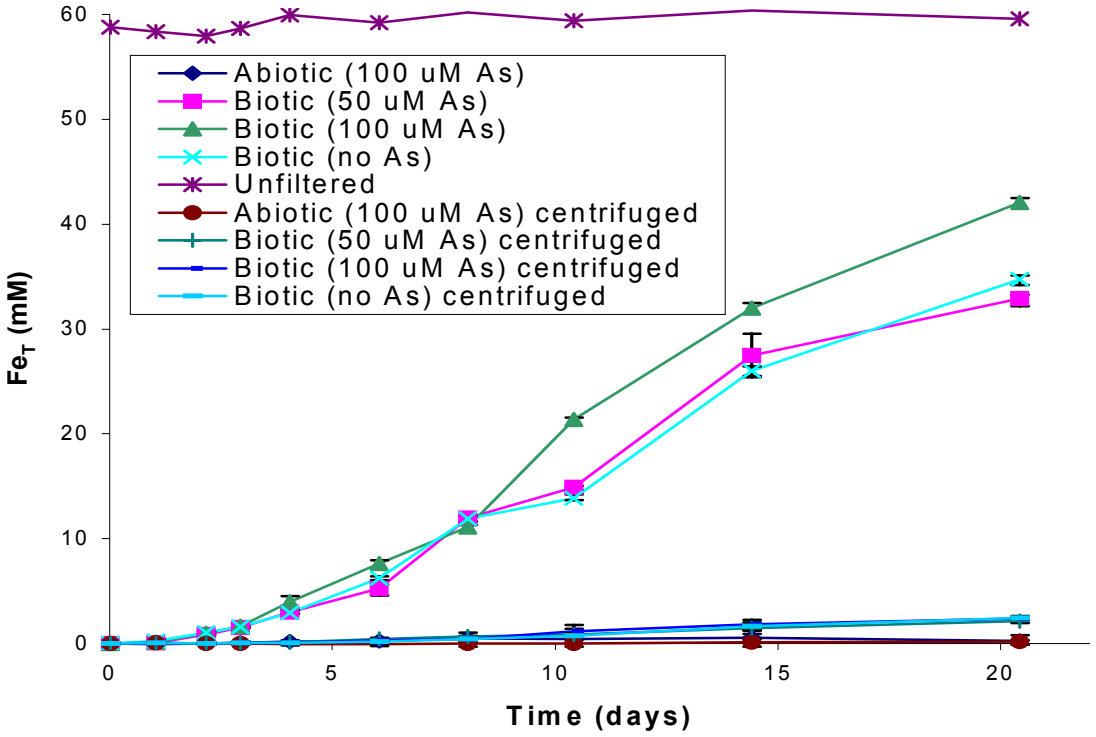

Figure 12: Fe_T present in filtered (0.2 micron), unfiltered, and filtered/ultracentrifuged samples. Results are shown as averages of triplicate experiments; error bars denote the maximum and minimum concentrations of total iron for each triplicate.

On day 20, the filtered and filtered/ultracentrifuged samples were analyzed for both Fe_T and Fe(II) (Figure 13; Appendix N). Fe_T in the biotic samples decreased substantially after the samples were centrifuged, while the abiotic Fe_T and Fe(II)

concentrations remained constant. These results indicate that the majority of the Fe(II) present in the filtered samples is associated with the iron nanoparticles that can be removed via ultra-centrifugation, and not as hydrated ions.

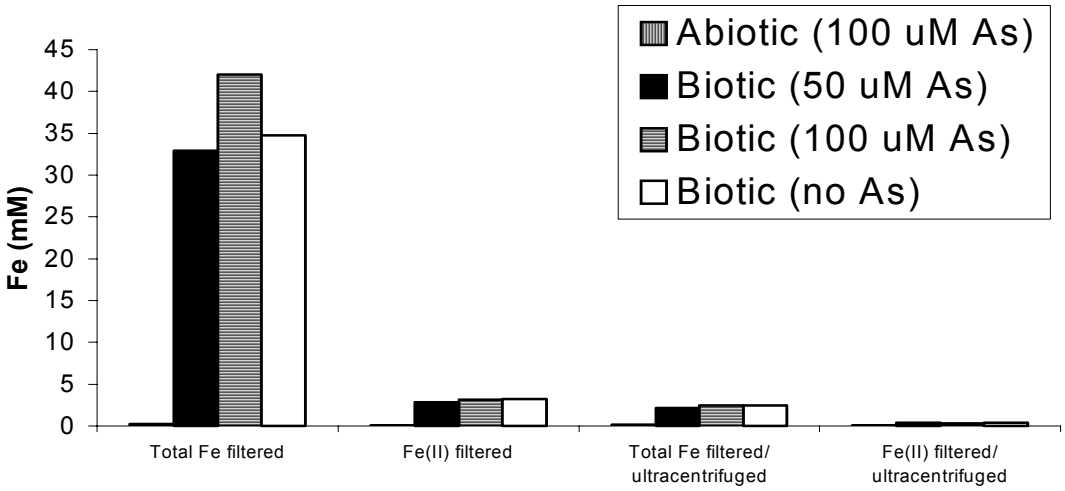

Figure 13: Total Fe and Fe(II) in the filtered and filtered/ultracentrifuged samples on day 20.

Arsenic Mobilization

Results of the arsenic analysis on filtered and filtered/ultracentrifuged samples are shown in Figure 14 (Appendix O). Results of analysis of filtered samples show that arsenic was mobilized in the biotic trials but not the abiotic control, indicating a connection between arsenic mobilization and biotic activity. The microcosms that contained 100 μM arsenic had approximately twice as much arsenic in the filtered samples than the microcosms that contained 50 μM arsenic, showing that loading rate of arsenic on the iron gel plays a critical role on how much arsenic is mobilized.

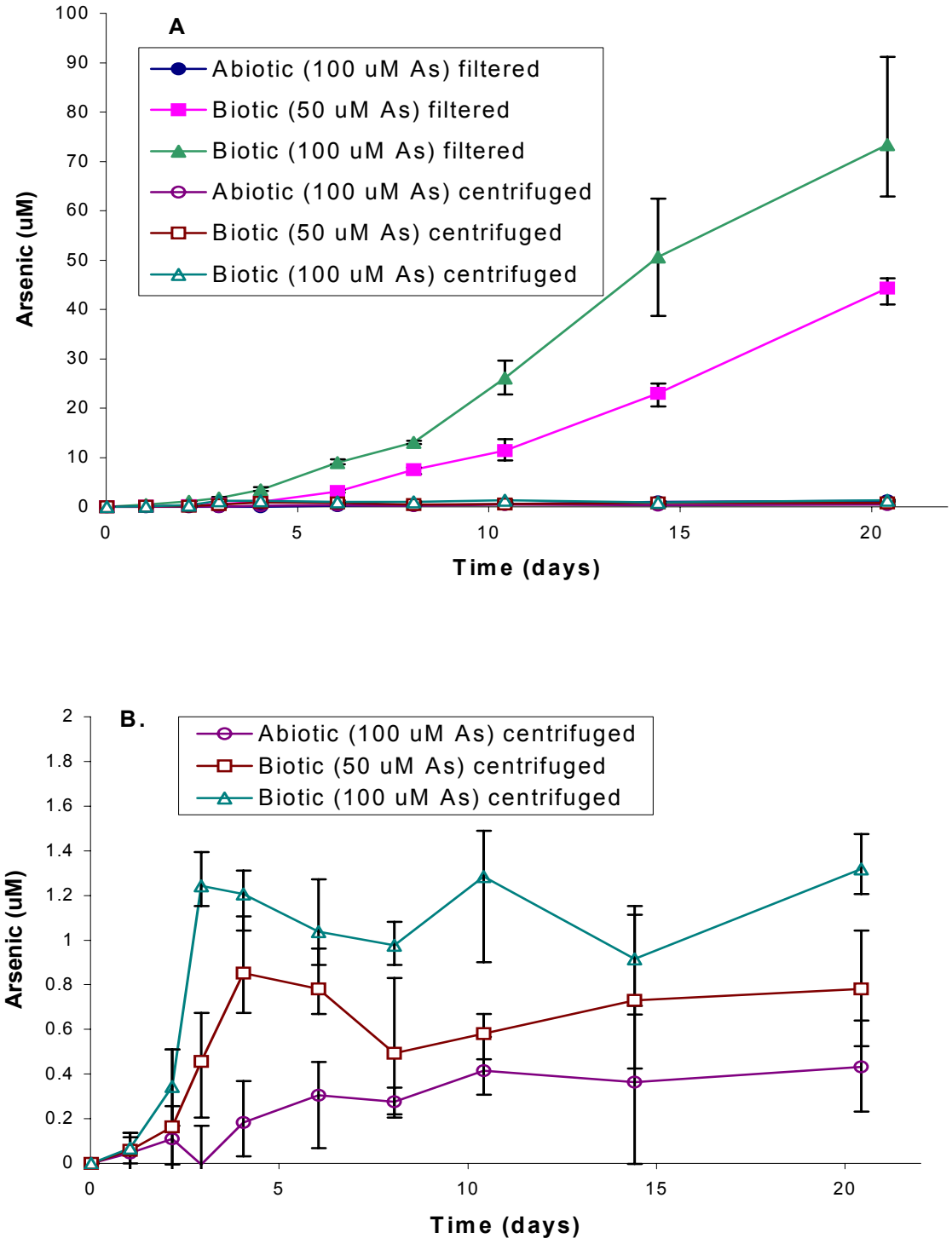

Figure 14: A. Arsenic in filtered and filtered/ultracentrifuged samples. B. Arsenic in filtered/ultracentrifuged samples only. Results shown as averages of triplicate experiments; error bars denote maximum and minimum arsenic concentrations for each triplicate.

As arsenic speciation has been shown to be an important control on mobilization, an arsenic speciation analysis was performed on filtered samples collected from day 20 (data not shown). Results indicate that all of the arsenic present in the filtered samples was arsenate, confirming previous studies documenting that GS-15 is unable to reduce arsenate to arsenite (Ahmann et al., 1997).

Phase Distribution of Arsenic

Comparison of arsenic concentrations in the filtered and filtered/ultracentrifuged samples (Figure 14a) shows that arsenic concentrations of the filtered samples are significantly higher than those in the filtered/ultracentrifuged samples. By day 20, centrifuged samples collected from the biotic trials contained less than 2% of the arsenic present in the filtered-only samples. Because the majority (~98%) of arsenic was removed by ultracentrifugation, these results indicate that the arsenic mobilized in the biotic experiments was not present as hydrated oxyanions but instead was associated with nanoparticles. However, it is interesting to note that in the filtered/ultracentrifuged samples (Figure 14b), arsenic concentrations increased during the first 5 days, and then stabilized.

To further examine the extent to which mobilized arsenic was associated with iron nanoparticles, the ratios of total iron in filtered samples to total iron in the media and arsenic in filtered samples to total arsenic in the media were calculated (Figure 15; Appendix P). As time progresses, the fraction of arsenic that passes through the filter is directly proportional to the fraction of iron that passes through the filter. These results support the hypothesis that the arsenic measured after filtration is bound to iron

nanoparticles that can pass through the 0.2 micron membrane, but are removed during ultra-centrifugation.

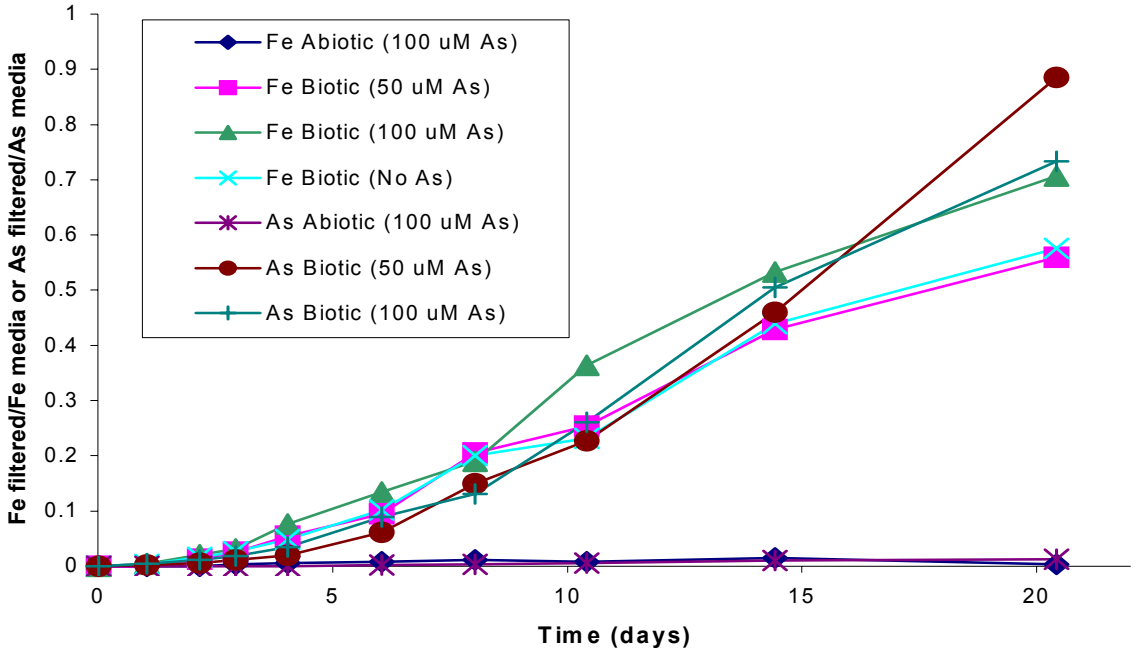

Figure 15: Ratio of iron and arsenic that passed through a 0.2 micron membrane to the total iron (0.056 M) and arsenic (50 or 100 μM) in the media.

Mechanisms of Arsenic Mobilization

Results of this experiment showed that arsenic was readily mobilized due to microbial activity and that the mobilized arsenic was removed from solution by ultracentrifugation. These results suggest that the dominant mechanism for arsenic mobilization by GS-15 is by dispersion of aggregated iron nanoparticles. There are two possible causes for microbially-mediated disaggregation of the iron oxide nanoparticles: organic coating of nanoparticles or phase transformation of ferrihydrite to magnetite (a mixed Fe(II)/Fe(III) mineral). Both of these could cause changes in the surface charge of

the nanoparticles, which could induce disaggregation. Because there was abundant acetate (0.08 M) in both the biotic and abiotic trials and disaggregation of nanoparticles was only occurring in the biotic trials, it is unlikely that the mechanism for disaggregation of nanoparticles was due to the formation of an organic coating on the nanoparticles. Even if GS-15 was producing organic molecules in the biotic trials, the high concentration of acetate present in the microcosm would out-compete these organic molecules for surface sites. Disaggregation of iron nanoparticles due to the phase transformation of ferrihydrite to magnetite is likely occurring because magnetite was identified in the biotic trials by TEM analysis. This phase transformation from ferrihydrite to magnetite would cause disaggregation of nanoparticles because magnetite has a lower point of zero charge (pzc) than ferrihydrite (McBride, 1994). This means that at the neutral pH of the microcosm, the surface charge of the magnetite would be much more negative than ferrihydrite, and the nanoparticles would be disaggregated due to electrostatic effects.

Although disaggregation was shown to be the dominant arsenic mobilization mechanism in this research, it appears that arsenic release as hydrated oxyanions might be a factor during the first 5 d after inoculation, as suggested by the similarity in arsenic concentrations in the filtered samples before and after ultracentrifugation. This means that either the arsenic is being released from the surface of the iron oxide nanoparticles or the arsenic is associated with iron nanoparticles that are not removed from suspension via ultracentrifugation.

Implications

Under the experimental conditions of this study, the dominant mechanism for arsenic mobilization due to microbially-mediated Fe(III) reduction is the disaggregation of arsenic-bearing ferrihydrite nanoparticles, and not release of arsenic oxyanions to solution. These results have significant implications for arsenic release and transport within aquifer systems. Particles with diameters less than 10 micrometers are widely recognized as mobile in both the unsaturated and saturated zones of the subsurface (Huling, 1989). However, these particles are often not considered in contaminant transport models. Transport models that assume arsenic will be adsorbed to an immobile iron phase and do not consider transport of arsenic-bearing particles may severely underestimate arsenic mobility in aquifers. This result has significant implications for human health, as arsenic-bearing iron (hydr)oxide nanoparticles ingested with drinking water can be easily dissolved by stomach acids, releasing arsenic to the body.

Conclusion

A series of controlled laboratory experiments was conducted to examine the impact of microbial activity on arsenic mobilization under iron reducing conditions. To accomplish this, a ferrihydrite and media slurry was loaded with arsenic and inoculated with *Geobacter metallireducens*, an iron-reducing microorganism. The phase distribution (solid vs. solution) of iron and arsenic was determined through filtration and ultracentrifugation techniques.

Under the experimental conditions of this study, the dominant mechanism for arsenic mobilization by *Geobacter metallireducens* is disaggregation of arsenic-bearing

iron oxide nanoparticles. The mechanism of this disaggregation of nanoparticles was most likely microbially mediated phase transformation of ferrihydrite to magnetite. Release of hydrated arsenic oxyanions may occur during the first 5 d of microbial growth, but is significantly overshadowed by disaggregation. Abiotic controls showed no significant increase in arsenic, indicating that arsenic mobilization was due to microbial activity and not due to abiotic processes such as competitive desorption. The presence of arsenic had no inhibitory effects on the growth of *Geobacter metallireducens*. These results provide an important insight into arsenic mobilization in iron reducing environments and may aid in improving future efforts for monitoring and remediation of arsenic-contaminated waters.

References

Ahmann, D., L. R. Krumholz, H. Hemond, D. Lovley, and F. Morel (1997). "Microbial mobilization of arsenic from sediments of the Aberjona Watershed." Environmental Science & Technology **31**(10): 2923-2930.

Ahmann, D., A. L. Roberts, L. Krumholz, and F. Morel (1994). "Microbe grows by reducing arsenic." Nature **371**(6500): 750.

Ahmed, K., P. Bhattacharya, M. Hasan, S. Akhter, S. Alam, M. Bhuyian, M. Imam, A. Khan, and O. Sracek (2004). "Arsenic enrichment in groundwater of the alluvial aquifers in Bangladesh: an overview." Applied Geochemistry **19**(2): 181-200.

Akai, J., K. Izumi, H. Fukuhara, H. Masuda, S. Nakano, T. Yoshimura, H., Ohfuji, H. Ananwar, and K. Akai (2004). "Mineralogical and geomicrobial investigations on groundwater arsenic enrichment in Bangladesh." Applied Geochemistry **19**(2): 215-230.

Andreae, M. (1983). Biotransformation of arsenic in the marine environment. Arsenic: Industrial, biomedical, environmental perspectives. W. Lederer and R. Fensterheim. New York, Van Nostrand Reinhold.

Andreae, M. (1986). Organometallic compounds in the environment: Principles and Reactions. P. J. Craig. New York, John Wiley & Sons.

Barrow, N. (1974). "On the displacement of adsorbed anions from soil: 2. Displacement of phosphate by arsenate." Soil Science **117**: 29-33.

Chiu, V. Q. and J. G. Hering (2000). "Arsenic adsorption and oxidation at manganite surfaces. 1. Method for simultaneous determination of adsorbed and dissolved arsenic species." Environmental Science & Technology **34**(10): 2029-2034.

Chouchane, S. and E. T. Snow (2001). "In vitro effect of arsenical compounds on glutathione related enzymes." Chemical Research in Toxicology **14**(5): 517-522.

Cornell, R. M. and U. Schwertmann (1996). The iron oxides; structure, properties, reactions, occurrences, and uses. VCH Verlagsgesellschaft, Weinheim, Federal Republic of Germany.

Cullen, W. and K. Reimer (1989). "Arsenic speciation in the environment." Chem. Rev. **89**: 713-764.

Cummings, D. E., F. Caccavo, S. Fendorf, and R. F. Rosenzweig (1999). "Arsenic mobilization by the dissimilatory Fe(III)-reducing bacterium Shewanella alga BrY." Environmental Science & Technology **33**(5): 723-729.

Davis, A., D. Sherwin, R. Ditmars, and K. Hoenke (2001). "An analysis of soil arsenic records of decision." Environmental Science & Technology **35**(12): 2401-2406.

Dixit , S. and J.G. Hering (2003). "Comparison of arsenic(V) and arsenic (III) sorption onto iron oxide minerals: Implications for arsenic mobility." Environmental Science & Technology **37** (18): 4182-4189.

Dzombak, D. and F. Morel (1990). Surface Complexation Modeling: Hydrous Ferric Oxide. New York, Wiley.

Eary L. E. and Schramke J. A. (1990) Rates of inorganic oxidation reactions involving dissolved- oxygen. ACS Symposium Series **416**: 379-396.

EPA (2001). Fact Sheet: Drinking Water Standard for Arsenic (EPA 815-F-00-015). Washington DC, EPA.

Fuller, C. C., J. A. Davis, and G. Waychunas (1993). "Surface-Chemistry of Ferrihydrite .2. Kinetics of Arsenate Adsorption and Coprecipitation." Geochimica et Cosmochimica Acta **57**(10): 2271-2282.

Garbarino J., Bednar A., and Burkhardt M. (2002) Methods of analysis by the U.S. Geological Survey National Water Quality Laboratory - Arsenic Speciation in Natural Water Samples, pp. 40. U.S. Geological Survey Water-Resources Investigation Report WRI 02-4144.

Gihring, T. M., G. K. Druschel, R. McCleskey, R. Hamers, and J. Banfield (2001). "Rapid arsenite oxidation by Thermus aquaticus and Thermus thermophilus: Field and laboratory investigations." Environmental Science & Technology **35**(19): 3857-3862.

Glasauer, S., P. G. Weidler, S. Langley, and T. Beveridge (2003). "Controls on Fe reduction and mineral formation by a subsurface bacterium." Geochimica et Cosmochimica Acta **67**(7):1277-1288.

Goldberg, S. (2002). “Competitive adsorption of arsenate and arsenite on oxides and clay minerals.” Soil Science Society of America Journal **66**:413-421.

Greffie, C., M. Amouric, and C. Parron (2001). "HRTEM study of freeze-dried and untreated synthetic ferrihydrites: consequences of sample processing." Clay Minerals **36**: 381-387.

Holm, T., M. Anderson, D. Iverson, and R. Stanforth (1979). "Heterogeneous interactions of arsenic in aquatic systems." Chemical Modeling in Aqueous Systems. J. EA. Washington DC, American Chemical Society.

Huling, S. G. (1989). "Superfund Ground Water Issue: Facilitated Transport (EPA/540/4-89/003)." Washington DC, EPA.

Islam, F., A. Gault, C. Boothman, D. Polya, J. Charnock, D. Chatterjee, and J. Llyod (2004). "Role of metal-reducing bacteria in arsenic release from Bengal delta sediments. Nature **430**: 68-71.

Janney, D., Cowley, J., Buseck, P. (2000). "Transmission Electron Microscopy of Synthetic 2- and 6-Line Ferrihydrite." Clays and Clay Minerals **48**(1): 111-119.

Knowles, F. and A. Benson (1983). "Trends in Biochem Sci." Biochem Sci **8**: 178-180.

Kukkadapu, R., J. Zachara, J. Fredrickson, and D. Kennedy (2004). "Biotransformation of two-line silica-ferrihydrite by a dissimilatory Fe(III)-reducing bacterium: Formation of carbonate green rust in the presence of phosphate." Geochimica et Cosmochimica Acta **68**(13):2799-2814.

Langner, H. and W. Inskeep (2000). "Microbial reduction of arsenate in the presence of ferrihydrite." Environmental Science & Technology **34**: 3131-3136.

Langner, H. W., C. R. Jackson, T. McDermott, and W. Inskeep (2001). "Rapid oxidation of arsenite in a hot spring ecosystem, Yellowstone National Park." Environmental Science & Technology **35**(16): 3302-3309.

Laverman, A. M., J. S. Blum, J. Schaefer, E. Philips, D. Lovley, and R. Oremland (1995). "Growth of strain ses-3 with arsenate and other diverse electron-acceptors." Applied and Environmental Microbiology **61**(10): 3556-3561.

Le, X.C., S. Yalcin, and M. S. Ma (2000). "Speciation of submicrogram per liter levels of arsenic in water: On-site species separation integrated with sample collection." Environmental Science & Technology **34** (11): 2342-2347

Lovley, D. R. and E. J. P. Phillips (1986). "Organic matter mineralization with reduction of ferric iron in anaerobic sediments." Applied and Environmental Microbiology **51**(4): 683-689.

Lovley, D. R. and S. Goodwin (1988). "Hydrogen concentrations as an indicator of the predominant terminal electron-accepting reactions in aquatic sediments." Geochimica et Cosmochimica Acta **52**: 2293-3003.

Lovley, D. R. (2000). "Environmental microbe-metal interactions." ASM Press, Washington, D.C.

Manning, B. A. and S. Goldberg (1996). "Modeling arsenate competitive adsorption on kaolinite, montmorillonite and illite." Clays and Clay Minerals **44**(5): 609-623.

McBride, M. B. (1994). "Environmental Chemistry of Soils." Oxford University Press, NY, NY.

Moore, J. N., W. H. Ficklin, and C. Johns (1988). "Partitioning of arsenic and metals in reducing sulfidic environments." Environmental Science & Technology **22**: 432-437.

Newman, D. K., E. K. Kennedy, J. Coates, D. Ahmann, D. Ellis, D. Lovley, and F. Morel (1997). "Dissimilatory arsenate and sulfate reduction in Desulfotomaculum auripigmentum sp. nov." Archives of Microbiology **168**(5): 380-388.

Nickson, R., J. McArthur, W. Burgess, K. Ahmed, P. Ravenscroft, and M. Rahman (1998). "Arsenic poisoning of Bangladesh groundwater." Nature **395**(6700): 338.

Nickson, R., J. McArthur, P. Ravenscroft, W. Burgess, and K. Ahmed (2000). "Mechanism of arsenic release to groundwater, Bangladesh and West Bengal." Applied Geochemistry **15**(4): 403-413.

NRC (1999). Arsenic in Drinking Water. Washington DC, National Academy Press.

Oremland, R. S. and J. F. Stolz (2003). "The ecology of arsenic." Science **300**: 939-943.

Peterson M. and Carpenter R. (1986) "Arsenic distribution in porewaters and sediments of Puget Sound, Lake Washington, the Washington Coast and Saanich Inlet, B.C." Geochimica et Cosmochimica Acta **50**, 353-369.

Pierce, M. and C. Moore (1980). "Adsorption of arsenite on amorphous iron hydroxide from dilute aqueous solution." Environmental Science & Technology **14**: 214-216.

Raven, K. P., A. Jain, and R. Loeppert (1998). "Arsenite and arsenate adsorption on ferrihydrite: Kinetics, equilibrium, and adsorption envelopes." Environmental Science & Technology **32**(3): 344-349.

Roy, W., J. Hassett, and R. Griffin (1986). "Competitive interactions of phosphate and molybdate on arsenate adsorption." Soil Science **142**: 203-210.

Schreiber ME, Simo JA, and PG Freiberg. (2000). "Stratigraphic and geochemical controls on naturally-occurring arsenic in groundwater, Eastern Wisconsin, USA". Hydrogeology Journal 8: 161-176.

Schwertmann, U. and R. M. Cornell (1991). Goethite. Iron Oxides in the Laboratory: Preparation and Characterization. Weinheim, VCH**:** 61-80.

Sen, C. K. (1997). "Nutritional Biochemistry of cellular glutathione." Nutritional Biochemistry **8**: 660-672.

Smedley, P. L. and D. G. Kinniburgh (2002). "A review of the source, behaviour, and distribution of arsenic in natural waters." Applied Geochemistry **17**: 517-568

Smith, A., P. Lopipero, M. Bates, and C. Steinmaus (2002). "Arsenic epidemiology and drinking water standards." Science **296**: 2145-2146.

Stollenwerk, K. (2003). Geochemical processes controlling transport of arsenic in groundwater: A review of adsorption. Pages 67-100 *in* A. Welch and K. Stollenwerk, editors. Arsenic in Groundwater. Kluwer Academic Publishers, Boston.

Stookey, L. (1970). "Ferrozine-a new spectrophotometric reagent for iron." Analytical Chemistry **42**: 779-781.

Stuben, D., Z. Berner, D. Chandrasekharam, and J. Karmakar (2003). "Arsenic enrichment in groundwater of West Bengal, India: geochemical evidence for mobilization of As under reducing conditions." Applied Geochemistry **18**: 1417-1434.

Welch, A. H., M. S. Lico, and J. Hughs (1988). "Arsenic in Ground-Water of the Western United-States." Ground Water **26**(3): 333-347.

Welch, A. H., D. B. Westjohn, D. Helsel, and R. Wanty (2000). "Arsenic in ground water of the United States: Occurrence and geochemistry." Ground Water **38**(4): 589-604.

Wilkie, J. A. and J. G. Hering (1996). "Adsorption of arsenic onto hydrous ferric oxide: effects of adsorbate/adsorbent ratios and co-occurring solutes." Colloids and Surfaces: Physiochemical and Engineering Aspects **107**: 97-110.

Wilkie, J. A. and J. G. Hering (1998). "Rapid oxidation of geothermal arsenic(III) in streamwaters of the eastern Sierra Nevada." Environmental Science & Technology **32**(5): 657-662.

Winship, K. A. (1984). "Toxicity of inorganic arsenic salts." Adverse Drug Reactions and Toxilogical Reviews **3** (3):129-160.

Witschi, A., S. Reddy, B. Stofer, and B. Lauterburg (1992). "The systemic availability of oral glutathione." Eur J Clin Pharmacol **43**: 667-669.

Zheng, Y., M. Stute, A. van Geen, I. Gavrieli, R. Dhar, H. J. Simpson, P. Schlosser, and K. Ahmed (2004). "Redox control of arsenic mobilization in Bangladesh groundwater." Applied Geochemistry **19**(2): 201-214.

Zobrist, J., P. R. Dowdle, J. Davis, and R. Oremland (2000). "Mobilization of arsenite by dissimilatory reduction of adsorbed arsenate." Environmental Science & Technology **34**(22): 4747-4753.

Appendices

Appendix A

Title: Ferrihydrite (Iron Gel) Synthesis

1. Dissolve 108g of ferric chloride hexahydrate in 1 L of Milli-Q water.
2. While constantly stirring add 10N NaOH dropwise to the solution to bring it up to pH 7.
3. Allow solution to equilibrate for 30 minutes and bring the pH back up to 7 with 10N NaOH.
4. Once pH is stable at 7 for 30 minutes, divide total volume into several 50mL centrifuge tubes.
5. Spin the centrifuge tubes at 10,000rpm for 15 minutes.
6. Remove the supernatant and resuspend precipitate in Milli-Q water.
7. Repeat steps 5 and 6 six times to fully desalt the iron oxide particles.
8. Combine iron gel in large plastic bottle.
9. Measure the concentration of iron in the iron gel (Ferrozine method) and adjust the solution accordingly to make it 1 M Fe.

Appendix B

Title: Procedure for loading iron gel media with arsenic

1. Remove iron gel media from the anaerobic chamber and put 400mL in a PPE bag
2. Place the bag in the titration vessel and clamp down top.
3. Hook-up the ultrapure nitrogen, titrator, pH probe, and impeller to the titration vessel.
4. Fill pH stat titration bottle with 0.1N HCl.
5. Set endpoint to pH 7
6. Use the pH stat to adjust the initial media pH to 7 and maintain it for 2 hours.
7. Add desired amount of arsenate from sodium arsenate stock solution.
8. Activate pH stat again to return the pH to 7 and let it stabilize for 2 hours.
9. Quickly remove the bag and re-introduce into the anaerobic chamber.
10. Allow media to equilibrate with the chamber atmosphere for 24hrs

Appendix C

Title: Sorption isotherm data for arsenate on ferrihydrite in the presence of 0.01M NaCl and in the presence of media

Data presented in Figures 3 and 4

Ferrihydrite in media

Total As concentration (uM)	As in solution (uM)	As sorbed (uM)	Ferrihydrite (g/L)	As sorbed (umol/g)	As sorbed (umol/m^2)
0.0000	0.0000	0.0000	2.3584	0.0000	0.0000
46.1993	0.0407	46.1586	2.3478	19.6599	0.0799
91.3120	0.0790	91.2330	2.3374	39.0318	0.1585
448.2442	0.2647	447.9795	2.3271	192.4990	0.7819
886.5210	1.1943	885.3267	2.3171	382.0815	1.5519
1746.3083	18.8856	1727.4227	2.3072	748.6947	3.0410
2596.6240	171.1923	2425.4317	2.2975	1055.6811	4.2879
5022.7248	2337.2432	2685.4816	2.2881	1173.6618	4.7672

Ferrihydrite in 0.01M NaCl

Total As concentration (uM)	As in solution (uM)	As sorbed (uM)	Ferrihydrite (g/L)	As sorbed (umol/g)	As sorbed (umol/m^2)
0.0000	0.0000	0.0000	2.3585	0.0000	0.0000
51.1267	0.0000	51.1267	2.3467	21.7864	0.0885
76.8867	0.0000	76.8867	2.3350	32.9280	0.1337
102.7896	0.0000	102.7896	2.3233	44.2432	0.1797
256.8928	0.0000	256.8928	2.3116	111.1299	0.4514
512.2581	0.0000	512.2581	2.3001	222.7118	0.9046
765.7204	0.0000	765.7204	2.2886	334.5743	1.3590
1017.4042	0.0000	1017.4042	2.2773	446.7620	1.8146
1507.3035	0.2470	1507.0566	2.2661	665.0371	2.7012
1986.1817	1.3656	1984.8161	2.2551	880.1266	3.5749
2907.8115	11.3466	2896.4650	2.2445	1290.4793	5.2416
3806.0314	108.3930	3697.6384	2.2341	1655.1117	6.7227
4688.4811	419.5556	4268.9255	2.2239	1919.6061	7.7970
5578.6474	1002.5016	4576.1458	2.2138	2067.1274	8.3962
7327.4174	2623.0567	4704.3607	2.2039	2134.5797	8.6702
9051.7152	4333.0494	4718.6657	2.1942	2150.5645	8.7351

Notes:
1. Samples were filtered though a 0.2 micron membrane, preserved with 2 N HCl, and analyzed by GFAA.
2. Total arsenic concentration (uM) = calculated by dividing the total mols of arsenic added by the total volume of the solution.

3. Arsenic in solution (uM) = filtered with 0.2 micron membrane and analyzed by GFAA.
4. Arsenic sorbed (uM) = calculated by subtracting As in solution from the total arsenic concentration
5. Ferrihydrite (g/L) = calculated by multiplying by the dilution factor after acidification to pH 7 and then subtracting the amount of ferrihydrite removed in each sample.
6. Arsenic sorbed (umol/g) = calculated by dividing the arsenic sorbed in uM by the ferrihydrite concentration in g/L.
7. Arsenic sorbed (umol/m^2) = calculated by dividing the arsenic sorbed in umol/g by the determined surface area of ferrihydrite, 245g/m^2.

Appendix D

Title: Anaerobic water procedure

1. Boil 1 L of Milli-Q water for 20minutes.
2. Sparge water with deoxygenated nitrogen gas for 45min.
3. Autoclave water for 45 minutes at 127^{o} C.
4. Sparge autoclaved water with deoxygenated nitrogen gas for 30min.
5. Place water in environmental chamber with atmosphere of 95%N_2 and 5%H_2.
6. Leave cap slightly ajar and mix the solution on a shaking table for 24 hrs.
7. After the water has been equilibrated with the atmosphere, tighten cap.
8. To test if the water is anoxic, use the resazurin method (clear = anoxic) or a dissolved oxygen probe (<1ppb O_2)

Appendix E

Title: Deoxygenated ultrapure nitrogen sparging method

1. Fill a 1 L sidearm flask with 400mL DI water
2. Dissolve 5 pellets of NaOH in the water
3. Sparge the basic water with ultrapure nitrogen for 15min
4. Add ~0.5g of sodium dithionite to the solution
5. Sparge with ultrapure nitrogen for 15min
6. Add ~0.1g of methyl viologen to the solution
7. Sparge with ultrapure nitrogen for 5 more minutes
8. By running the ultrapure nitrogen through this solution it will be deoxygenated and can be used for anaerobic media preparation.

Appendix F

Title: Resazurin: oxygen indicator procedure

(Blue=Oxic / Bright Pink or Clear = Anoxic)

Stock Solution (1g/L):
1. Fill 100mL serum vial with milli-q water
2. Cover top with foil
3. Autoclave for about 40 minutes
4. As cooling, sparge with N_2 gas
5. Put on septa and crimp

6. Fill 100mL volumetric flask partway with milli-q water
7. Weigh out 0.1g resazurin
8. Add to flask, rinse weigh boat with milli-q water
9. Bring to volume with milli-q water
10. Mix
11. Put in plastic bottle
12. Add 0.1mL of resazurin solution per 100mL of desired solution.

E'o = -51mv
Should be colorless at -110mv

Reference:
Ljungdahl, L and Weigel, J. 1986. Working with anaerobic bacteria. In Manual of Industrial Microbiology. Demain AL and Solomon NA, editors. ASM Press. P. 84-96.

Appendix G

Title: *Geobacter metallireducens* media recipe

ATCC Medium: #1768 Broth Recipe

In 1L of milli-q water combine:

- Ferric citrate 13.70g
- Vitamin solution (see below), 10mL
- Mineral solution (see below), 10mL
- $NaHCO_3$, 2.50g
- NH_4Cl, 0.25g
- $NaH_2PO_4 \cdot H_2O$, 0.06g (1/10 of recommended amount)
- KCl, 0.1g
- Sodium acetate, 6.8g

  Heat about 400mL of Milli-Q water on a hot/stir plate to near boiling. Add ferric citrate, allow it to dissolve then cool to room temperature in a slurry of ice, bring the volume of Milli-Q water up to 800mL by adding 400mL of Milli-Q water. Adjust the pH to 6.0 using 10N NaOH.
  Add the remaining ingredients and bring the final volume up to 1 L with Milli-Q water. Sparge the media with deoxygenated ultrapure nitrogen. The final pH should be between 6.8 and 7.0. Cover media bottle with aluminum foil to prevent exposure to sunlight.
  **When making iron gel media, do not add ferric citrate and add enough synthesized ferrihydrite to make the iron concentration of the media 0.056M Fe. Do not expose iron gel media to heat to prevent transformation of ferrihydrite.*

Wolfe's Vitamin Solution

- Biotin, 2.0mg
- Folic acid, 2.0 mg
- Pyridoxine hydrochloride, 10.0 mg
- Thiamine . HCl, 5.0mg
- Riboflavin, 5.0mg
- Nicotinic acid, 5.0mg
- Calcium D-(+)-pantothenate, 5.0mg
- Vitamin B_{12}, 0.1 mg
- P-Aminobenzoic acid, 5.0mg
- Thioctic acid, 5.0mg
- Distilled water, 1.0 L

  Cover vitamin solution bottle with aluminum foil to prevent photodegradation of chemicals.

Wolfe's Mineral Solution

- $NiCl_2 \cdot 6H_2O$, 24.0mg
- Na_2WO_4, 25.0mg
- Nitrilotriacetic acid, 1.5g
- $MgSO_4 \cdot 7H_2O$, 3.0g
- $MnSO_4 \cdot H_2O$, 0.5g
- NaCl, 1.0g
- $FeSO_4 \cdot 7H_2O$, 0.1g
- $CoCl_2 \cdot 6H_2O$, 0.1g
- $CaCl_2$, 0.1g
- $ZnSO_4 \cdot 7H_2O$, 0.1g
- $CuSO_4 \cdot 5H_2O$, 0.01g
- $AlK(SO_4)_2 \cdot 12H_2O$, 0.01g
- H_3BO_3, 0.01g
- $Na_2MoO_4 \cdot 2H_2O$, 0.01g
- Distilled water, 1.0L
  Add nitriloacetic acid to 500mL of water and adjust to pH 6.5 with KOH to dissolve the compound. Bring volume to 1.0L with remaining water and add remaining compounds one at a time.

Appendix H

Title: Ferrozine method

1. Add 1g of ferrozine to 1L of 50mM HEPES to prepare ferrozine solution.
2. To a cuvette, add 1.5 ml ferrozine and 200 ul sample. Mix with pipette tip. Let sit for 15 minutes for color to develop. Make sure there are no bubbles. Read absorbance at a wavelength of 562nm (this is FeII).
3. Add 150 ul hydroxylamine HCl to the cuvette, swirl, wait 5 minutes, and read the absorbance (this is for total Fe).
4. Run water blanks in every 10 samples and make sure to record absorbance values. Run a replicate for every 20 samples.

Appendix I

Title: Fe(II) data for biotic ferric citrate media

Data presented in Figure 6

Time after inoculation (days)	Fe(II) produced (mM)
0.02	0.0000
0.06	-0.0752
0.15	0.1148
0.33	0.5622
0.81	1.0729
0.94	1.2947
1.15	1.9796
1.24	2.1657
1.45	2.7952
1.91	4.6798
2.11	6.8692
2.44	9.3279
2.85	20.2276
3.28	32.9605
3.80	35.1420
3.99	38.7449
4.32	43.5830
4.83	37.2206
4.97	36.1991
5.12	34.2037
5.72	27.6987

Notes:
1. Samples were filtered through a 0.2 micron membrane, preserved with 10 uL of 2 N HCl, and analyzed using the ferrozine method.
2. Fe(II) production was measured by absorbance and converted to mM of Fe(II) through a standard calibration curve.
3. Data were normalized by subtracting the concentration of Fe(II) present in the first sample taken immediately after inoculation.

Appendix J

Title: Fe(II) data for growth curves in biotic and abiotic iron gel medias.

Data presented in Figure 8

Key:
Trials A-F: Biotic iron gel media (6 replicates)
Trial G: Abiotic iron gel media

Time (days)	A (mM)	B (mM)	C (mM)	D (mM)	E (mM)	F (mM)
0.0000	0.0000	0.0000	0.0000	0.0000	0.0000	0.0000
1.0556	1.5060	1.1882	1.1462	1.0258	1.0842	1.5165
2.1076	2.4103	2.6627	2.5190	2.3204	2.0610	2.2608
2.8264	3.4805	3.7528	4.1886	2.8485	2.8041	3.2305
3.9306	4.4620	4.7319	4.2972	3.0880	3.4455	3.6873
5.0972	4.6851	5.1127	4.9480	4.2470	3.6967	4.0647
7.0972	5.2938	5.3581	5.6584	4.1243	4.2961	4.6898

Time (days)	G (mM)	Biotic Average (mM)	"+ error"	"- error"
0.0000	0.0000	0.0000	0.0000	0.0000
1.0556	0.1589	1.2445	0.2720	0.2187
2.1076	0.2243	2.3724	0.2903	0.3114
2.8264	0.3377	3.3842	0.8044	0.5801
3.9306	0.2676	3.9520	0.7799	0.8640
5.0972	0.1355	4.4590	0.6537	0.7624
7.0972	0.2068	4.9034	0.7550	0.7791

Notes:
1. Samples were unfiltered, digested with 0.5 N HCl, and analyzed using the ferrozine method.
2. Fe(II) production was measured by absorbance and converted to mM of Fe(II) through a standard calibration curve.
3. Data were normalized by subtracting the concentration of Fe(II) present in the first sample taken immediately after inoculation.
4. +/- errors were determined by calculating the difference between either the maximum or minimum value and the average value at each sampling time.

Appendix K

Title: Relative peak areas of hydrogen in biotic and abiotic trials of ferric citrate and iron gel media 1 week and 9 weeks after inoculation

Data presented in Figure 10

Hydrogen	Ferric Citrate Abiotic	Ferric Citrate Biotic	Iron Gel Abiotic	Iron Gel Biotic
1 week	10889923	7398150	10767987	9414040
9 weeks	9531100	5230735	9543551	4502236

Notes:
1. Samples were collected from the headspaces of the sealed microcosms and were analyzed on a gas chromatograph with a reductive gas detector.
2. Values represent relative peak areas for hydrogen.

Appendix L

Title: Total Fe(II) produced in microcosm slurry.

Data presented in Figure 11

Key:

A = Abiotic trials with 100uM loaded As (3 replicates)

B = Biotic trials with 50uM loaded As (3 replicates)

C = Biotic trials with 100uM loaded As (3 replicates)

D = Biotic trials with no As (3 replicates)

Time (d)	A1(mM)	A2(mM)	A3(mM)	A avg	B1 (mM)	B2 (mM)	B3 (mM)	B avg
0.02	0.0000	0.0000	0.0000	0.0000	0.0000	0.0000	0.0000	0.0000
1.04	0.0152	0.0152	0.0456	0.0253	0.3774	0.4615	1.1462	0.6617
2.17	-0.0093	-0.0304	-0.1554	-0.0650	1.4581	1.3354	2.2958	1.6965
2.94	-0.2278	-0.1484	-0.1636	-0.1799	2.3893	2.5809	3.0821	2.6841
4.04	-0.2255	-0.0759	-0.0421	-0.1145	3.1394	3.6955	4.2972	3.7107
6.04	-0.1741	-0.1005	-0.1250	-0.1332	3.7446	4.5414	4.9258	4.4039
8.04	-0.1332	-0.0444	-0.0549	-0.0775	4.6524	4.4596	4.6524	4.5881
10.42	-0.1344	-0.0526	-0.1624	-0.1164	5.1817	5.4235	5.4960	5.3671
14.42	-0.1227	0.0876	0.0783	0.0144	5.0683	5.0286	5.2857	5.1275
20.42	-0.1215	0.0549	-0.0316	-0.0327	4.7470	5.5555	5.8149	5.3725

Time (d)	C1(mM)	C2 (mM)	C3 (mM)	C avg	D1(mM)	D2 (mM)	D3 (mM)	D avg
0.02	0.0000	0.0000	0.0000	0.0000	0.0000	0.0000	0.0000	0.0000
1.04	0.4802	0.5924	0.6765	0.5830	0.3423	0.3937	0.5573	0.4311
2.17	1.7245	1.8098	1.9932	1.8425	1.2957	1.1765	1.3027	1.2583
2.94	3.6207	2.9349	2.9466	3.1674	2.1813	1.9944	2.2035	2.1264
4.04	4.3977	3.8731	3.8427	4.0378	3.0412	3.0658	3.1990	3.1020
6.04	5.7366	4.4316	4.0542	4.7408	3.5051	3.5039	3.7481	3.5857
8.04	5.7156	5.1747	4.8639	5.2514	3.6979	4.2330	4.2143	4.0484
10.42	6.8945	5.8313	5.4037	6.0431	4.6057	4.8288	4.9527	4.7957
14.42	6.5194	5.6362	5.2553	5.8036	4.5776	4.7611	4.9971	4.7786
20.42	7.1632	5.8523	5.5544	6.1900	4.7938	4.8464	5.3593	4.9998

Time (d)	A + error	A - error	B + error	B - error	C + error	C - error	D + error	D - error
0.02	0.0000	0.0000	0.0000	0.0000	0.0000	0.0000	0.0000	0.0000
1.04	0.0203	0.0101	0.4845	0.2843	0.0935	0.1028	0.1262	0.0888
2.17	0.0557	0.0904	0.5994	0.3610	0.1507	0.1180	0.0444	0.0818
2.94	0.0315	0.0479	0.3980	0.2948	0.4533	0.2325	0.0771	0.1320
4.04	0.0724	0.1110	0.5865	0.5713	0.3599	0.1951	0.0970	0.0608
6.04	0.0327	0.0409	0.5219	0.6593	0.9958	0.6866	0.1624	0.0818
8.04	0.0331	0.0557	0.0643	0.1285	0.4642	0.3875	0.1846	0.3505
10.42	0.0639	0.0460	0.1289	0.1854	0.8513	0.6395	0.1570	0.1901
14.42	0.0732	0.1371	0.1581	0.0989	0.7158	0.5484	0.2185	0.2010
20.42	0.0876	0.0888	0.4424	0.6255	0.9732	0.6356	0.3595	0.2060

Notes:
1. Samples were unfiltered, digested with 0.5 N HCl, and analyzed using the ferrozine method.
2. Fe(II) production was measured by absorbance and converted to mM of Fe(II) through a standard calibration curve.
3. Data were normalized by subtracting the concentration of Fe(II) present in the first sample taken immediately after inoculation.
4. +/- errors were determined by calculating the difference between either the maximum or minimum value and the average value at each sampling time.

Appendix M

Title: Total Fe in filtered, unfiltered, and filtered/ultracentrifuged samples.

Data presented in Figure 12

Key:

A = Abiotic trials with 100uM loaded As (3 replicates)

B = Biotic trials with 50uM loaded As (3 replicates)

C = Biotic trials with 100uM loaded As (3 replicates)

D = Biotic trials with no As (3 replicates)

Total Fe in filtered samples

Time (d)	A1(mM)	A2(mM)	A3(mM)	A avg	B1 (mM)	B2(mM)	B3(mM)	B avg
0.02	0.0000	0.0000	0.0000	0.0000	0.0000	0.0000	0.0000	0.0000
1.04	0.0044	-0.1980	-0.0638	-0.0858	-0.0704	0.1408	0.1210	0.0638
2.17	0.0154	-0.1848	0.1166	-0.0176	0.7569	1.0782	0.7415	0.8589
2.94	0.2046	-0.1386	0.1650	0.0770	1.4764	1.4830	1.5380	1.4992
4.04	0.3146	-0.0506	0.2046	0.1562	3.1927	2.8802	2.9858	3.0196
6.04	0.4907	-0.0110	0.3433	0.2743	5.6284	4.5965	5.4348	5.2199
8.04	0.6843	0.2882	0.4115	0.4613	12.1194	11.6617	12.0666	11.9492
10.42	0.4973	0.3609	0.4511	0.4364	15.0304	14.9314	14.6475	14.8698
14.42	0.8867	0.4291	0.3389	0.5515	25.4027	27.5128	29.5305	27.4820
20.42	0.2112	0.2816	0.2442	0.2457	33.1808	32.1775	33.2930	32.8838

Time (d)	C1(mM)	C2(mM)	C3(mM)	C avg	D1(mM)	D2(mM)	D3(mM)	D avg
0.02	0.0000	0.0000	0.0000	0.0000	0.0000	0.0000	0.0000	0.0000
1.04	0.2948	0.0726	0.0726	0.1467	0.1826	0.1430	0.4159	0.2472
2.17	1.2190	1.0209	0.7371	0.9923	0.9571	0.9439	1.1464	1.0158
2.94	1.8307	1.6876	1.4654	1.6612	1.5798	1.5446	1.7273	1.6172
4.04	4.5019	4.0332	3.3995	3.9782	2.8934	2.8164	3.1465	2.9521
6.04	7.9520	7.2038	7.6769	7.6109	6.0311	6.2335	6.4271	6.2306
8.04	11.2810	10.8696	11.2260	11.1256	11.8839	11.6155	12.1370	11.8788
10.42	21.5741	21.1957	21.2881	21.3526	13.7344	13.6464	14.2471	13.8760
14.42	31.5790	31.9706	32.4701	32.0066	26.0276	25.5325	26.4368	25.9990
20.42	41.9095	41.7269	42.4596	42.0320	34.1512	34.9719	35.1061	34.7431

Time (d)	A + error	A - error	B + error	B - error	C + error	C - error	D + error	D - error
0.02	0.0000	0.0000	0.0000	0.0000	0.0000	0.0000	0.0000	0.0000
1.04	0.0902	0.1122	0.0770	0.1342	0.1482	0.0741	0.1687	0.1041
2.17	0.1342	0.1672	0.2193	0.1174	0.2266	0.2552	0.1306	0.0719
2.94	0.1276	0.2156	0.0389	0.0227	0.1694	0.1958	0.1100	0.0726
4.04	0.1584	0.2068	0.1731	0.1394	0.5237	0.5787	0.1944	0.1357
6.04	0.2164	0.2853	0.4085	0.6234	0.3410	0.4071	0.1966	0.1995
8.04	0.2230	0.1731	0.1702	0.2875	0.1555	0.2560	0.2582	0.2633
10.42	0.0609	0.0755	0.1606	0.2222	0.2215	0.1570	0.3711	0.2296
14.42	0.3352	0.2127	2.0485	2.0793	0.4635	0.4276	0.4379	0.4665
20.42	0.0359	0.0345	0.4093	0.7063	0.4276	0.3051	0.3631	0.5919

Total Fe in unfiltered samples

Time (d)	Total Fe (mM)
0.02	58.8016
1.04	58.3654
2.17	57.9413
2.94	58.6589
4.04	59.9502
6.04	59.2365
8.04	60.1548
10.42	59.3685
14.42	60.3661
20.42	59.5893

Total Fe in filtered/ultracentrifuged samples

Time (d)	A1(mM)	A2(mM)	A3(mM)	A avg	B1 (mM)	B2(mM)	B3(mM)	B avg
0.02	0.0000	0.0000	0.0000	0.0000	0.0000	0.0000	0.0000	0.0000
1.04	0.0770	-0.0616	0.1056	0.0403	0.0638	-0.0066	0.0132	0.0235
2.17	-0.0330	0.0110	-0.0154	-0.0125	0.1320	-0.1232	0.0396	0.0161
2.94	0.0022	0.0242	-0.0220	0.0015	0.1980	-0.1144	0.0814	0.0550
4.04	0.0198	0.0022	-0.1914	-0.0565	0.2552	-0.0704	0.1452	0.1100
6.04	0.1870	-0.0330	-0.2706	-0.0389	0.5721	0.2882	0.4291	0.4298
8.04	0.2134	-0.0110	-0.2750	-0.0242	1.0540	0.4027	0.6315	0.6960
10.42	0.3873	0.0154	-0.3345	0.0227	1.4082	0.4335	0.7415	0.8611
14.42	0.4511	0.1584	-0.3147	0.0983	1.5292	1.2080	1.6150	1.4507
20.42	0.7767	-0.0836	-0.1408	0.1841	2.3279	1.9495	2.1651	2.1475

Time (d)	C1(mM)	C2(mM)	C3(mM)	C avg	D1(mM)	D2(mM)	D3(mM)	D avg
0.02	0.0000	0.0000	0.0000	0.0000	0.0000	0.0000	0.0000	0.0000
1.04	0.0022	0.0286	0.2134	0.0814	0.0682	0.0286	0.0660	0.0543
2.17	-0.1342	0.0506	0.0968	0.0044	-0.0814	0.0066	0.0880	0.0044
2.94	-0.0726	0.2134	-0.0066	0.0447	-0.0506	0.1584	0.0748	0.0609
4.04	0.0110	0.0352	0.1914	0.0792	-0.0770	0.1980	0.0396	0.0535
6.04	0.1584	0.3234	0.4115	0.2978	-0.0132	0.2926	0.2112	0.1636
8.04	0.2904	0.3124	0.7305	0.4445	0.1870	0.5193	0.5633	0.4232
10.42	0.5303	1.1244	1.7713	1.1420	0.4357	0.7481	0.9549	0.7129
14.42	1.3994	1.8637	2.2597	1.8409	1.2718	1.9979	1.6590	1.6429
20.42	2.2069	2.5942	2.4314	2.4108	2.4424	2.4402	2.4534	2.4453

Time (d)	A + error	A - error	B + error	B - error	C + error	C - error	D + error	D - error
0.02	0.0000	0.0000	0.0000	0.0000	0.0000	0.0000	0.0000	0.0000
1.04	0.0653	0.1019	0.0403	0.0301	0.1320	0.0792	0.0139	0.0257
2.17	0.0235	0.0205	0.1159	0.1394	0.0924	0.1386	0.0836	0.0858
2.94	0.0227	0.0235	0.1430	0.1694	0.1687	0.1174	0.0975	0.1115
4.04	0.0763	0.1350	0.1452	0.1804	0.1122	0.0682	0.1445	0.1306
6.04	0.2259	0.2318	0.1423	0.1416	0.1137	0.1394	0.1291	0.1768
8.04	0.2376	0.2508	0.3579	0.2934	0.2860	0.1540	0.1401	0.2362
10.42	0.3645	0.3572	0.5471	0.4276	0.6293	0.6117	0.2420	0.2772
14.42	0.3528	0.4129	0.1643	0.2428	0.4188	0.4415	0.3550	0.3711
20.42	0.5926	0.3249	0.1804	0.1980	0.1834	0.2039	0.0081	0.0051

Notes:
1. Filtered and filtered/ultracentrifuged samples were filtered through a 0.2 micron membrane, preserved with 2 N HCl, and analyzed using the ferrozine method.
2. Filtered/ultracentrifuged samples were spun at 109,000 rcf for 1 h.
3. Unfiltered samples were digested with 0.5N HCl and analyzed using the ferrozine method.
4. Data from the filtered and filtered/ultracentrifuged samples were normalized by subtracting the concentration of total iron present in the first sample taken immediately after inoculation.
5. +/- errors were determined by calculating the difference between either the maximum or minimum value and the average value at each sampling time.

Appendix N

Title: Total Fe (Fe(II) + Fe(III)) and Fe(II) in filtered and filtered/ultracentrifuged samples on day 20.

Data presented in Figure 13

Key:
A = Abiotic trials with 100uM loaded As (3 replicates)
B = Biotic trials with 50uM loaded As (3 replicates)
C = Biotic trials with 100uM loaded As (3 replicates)
D = Biotic trials with no As (3 replicates)

	A1(mM)	A2(mM)	A3(mM)	A avg	B1 (mM)	B2(mM)	B3(mM)	B avg
Total Fe filtered/ ultracentrifuged	0.7767	-0.0836	-0.1408	0.1841	2.3279	1.9495	2.1651	2.1475
Total Fe filtered	0.2112	0.2816	0.2442	0.2457	33.1808	32.1775	33.2930	32.8838
Fe(II) filtered/ ultracentrifuged	0.0896	0.0834	0.0944	0.0891	0.3023	0.3898	0.4168	0.3697
Fe(II) filtered	0.1146	0.1134	0.0724	0.1001	2.3713	2.8008	3.3286	2.8336

	C1(mM)	C2(mM)	C3(mM)	C avg	D1(mM)	D2(mM)	D3(mM)	D avg
Total Fe filtered/ ultracentrifuged	2.2069	2.5942	2.4314	2.4108	2.4424	2.4402	2.4534	2.4453
Total Fe filtered	41.9095	41.7269	42.4596	42.0320	34.1512	34.9719	35.1061	34.7431
Fe(II) filtered/ ultracentrifuged	0.3239	0.2879	0.2982	0.3033	0.3536	0.4056	0.3973	0.3855
Fe(II) filtered	3.1965	3.0660	3.1228	3.1284	3.0940	3.1673	3.3740	3.2118

Notes:
1. All samples were filtered through a 0.2 micron membrane, digested with 0.5 N HCl, and analyzed using the ferrozine method.
2. Filtered/ultracentrifuged samples were spun at 109,000 rcf for 1 h.
3. Data from the filtered and filtered/ultracentrifuged samples were normalized by subtracting the concentration of total iron or Fe(II) present in the first sample taken immediately after inoculation.

Appendix O

Title: Arsenic in filtered and filtered/ultracentrifuged samples

Data presented in Figure 14

Key:

A = Abiotic trials with 100uM loaded As (3 replicates)

B = Biotic trials with 50uM loaded As (3 replicates)

C = Biotic trials with 100uM loaded As (3 replicates)

D = Biotic trials with no As (3 replicates)

Arsenic in filtered samples

Time (d)	A1(uM)	A2(uM)	A3(uM)	A avg	B1 (uM)	B2 (uM)	B3 (uM)	B avg
0.02	0.0000	0.0000	0.0000	0.0000	0.0000	0.0000	0.0000	0.0000
1.04	-0.0395	-0.1046	0.0950	-0.0164	0.0723	0.2117	0.1204	0.1348
2.17	-0.0279	-0.0710	0.0444	-0.0182	0.2558	0.1999	0.3302	0.2620
2.94	-0.0444	-0.0159	0.1046	0.0148	0.5922	0.5327	0.6647	0.5965
4.04	0.0069	0.0081	0.1355	0.0502	1.0431	0.9853	1.0030	1.0105
6.04	0.3959	0.1347	0.2504	0.2603	2.8672	3.3806	2.9471	3.0650
8.04	0.4346	0.1839	0.2878	0.3021	7.8168	6.6638	7.9051	7.4619
10.42	0.2871	0.9569	0.4778	0.5739	10.8735	13.7157	9.4339	11.3410
14.42	1.0845	0.9142	0.9962	0.9983	25.0256	23.5660	20.3399	22.9772
20.42	1.2743	1.4685	0.9557	1.2328	46.2545	45.5076	41.0256	44.2625

Time (d)	C1 (uM)	C2 (uM)	C3 (uM)	C avg	D1 (uM)	D2 (uM)	D3 (uM)	D avg
0.02	0.0000	0.0000	0.0000	0.0000	0.0000	0.0000	0.0000	0.0000
1.04	0.3648	0.4788	0.3897	0.4111	0.0000	0.0000	0.0000	0.0000
2.17	1.0538	1.1229	1.1385	1.1051	0.0000	0.0000	0.0000	0.0000
2.94	1.9627	1.7907	1.7024	1.8186	0.0000	0.0000	0.0000	0.0000
4.04	3.9509	3.1876	3.2136	3.4507	0.0000	0.0000	0.0000	0.0000
6.04	9.6161	8.6175	8.6635	8.9657	0.0000	0.0000	0.0000	0.0000
8.04	13.3853	13.1516	12.7237	13.0869	0.0000	0.0000	0.0000	0.0000
10.42	29.6490	25.8169	22.7342	26.0667	0.0000	0.0000	0.0000	0.0000
14.42	62.4433	50.6108	38.6748	50.5763	0.0000	0.0000	0.0000	0.0000
20.42	91.1119	66.0109	62.9015	73.3414	0.0000	0.0000	0.0000	0.0000

Time (d)	A + error	A - error	B + error	B - error	C + error	C - error	D + error	D - error
0.02	0.0000	0.0000	0.0000	0.0000	0.0000	0.0000	0.0000	0.0000
1.04	0.1114	0.0883	0.0769	0.0625	0.0677	0.0463	0.0000	0.0000
2.17	0.0626	0.0529	0.0682	0.0621	0.0335	0.0513	0.0000	0.0000
2.94	0.0899	0.0592	0.0682	0.0638	0.1441	0.1162	0.0000	0.0000
4.04	0.0853	0.0432	0.0326	0.0252	0.5002	0.2631	0.0000	0.0000
6.04	0.1356	0.1256	0.3156	0.1977	0.6504	0.3481	0.0000	0.0000
8.04	0.1325	0.1182	0.4432	0.7981	0.2984	0.3632	0.0000	0.0000
10.42	0.3829	0.2868	2.3747	1.9071	3.5823	3.3325	0.0000	0.0000
14.42	0.0862	0.0841	2.0484	2.6372	11.8670	11.9015	0.0000	0.0000
20.42	0.2357	0.2771	1.9919	3.2370	17.7705	10.4399	0.0000	0.0000

As in filtered/ultracentrifuged samples

Time (d)	A1(uM)	A2(uM)	A3(uM)	A avg	B1 (uM)	B2 (uM)	B3 (uM)	B avg
0.02	0.0000	0.0000	0.0000	0.0000	0.0000	0.0000	0.0000	0.0000
1.04	0.1372	0.1105	-0.1105	0.0457	0.1216	-0.0808	0.1364	0.0591
2.17	0.0771	0.2566	-0.0045	0.1097	0.5094	-0.1594	0.1401	0.1634
2.94	0.1676	-0.0134	-0.1698	-0.0052	0.6740	0.2054	0.4879	0.4558
4.04	0.3688	0.1499	0.0326	0.1837	1.1068	0.6748	0.7732	0.8516
6.04	0.3943	0.4550	0.0696	0.3063	0.7161	0.6688	0.9631	0.7827
8.04	0.2843	0.3385	0.2051	0.2760	0.8297	0.2187	0.4342	0.4942
10.42	0.5672	0.3719	0.3086	0.4159	0.4655	0.6693	0.6113	0.5821
14.42	0.7049	0.3907	-0.0020	0.3645	1.1129	0.4249	0.6550	0.7309
20.42	0.6396	0.4266	0.2321	0.4328	1.0435	0.5243	0.7762	0.7813

Time (d)	C1 (uM)	C2 (uM)	C3 (uM)	C avg	D1 (uM)	D2 (uM)	D3 (uM)	D avg
0.02	0.0000	0.0000	0.0000	0.0000	0.0000	0.0000	0.0000	0.0000
1.04	0.0926	0.1163	-0.0003	0.0695	0.0000	0.0000	0.0000	0.0000
2.17	0.3514	0.1682	0.5113	0.3436	0.0000	0.0000	0.0000	0.0000
2.94	1.1804	1.1529	1.3945	1.2426	0.0000	0.0000	0.0000	0.0000
4.04	1.2631	1.0434	1.3120	1.2061	0.0000	0.0000	0.0000	0.0000
6.04	1.2722	0.9487	0.8897	1.0369	0.0000	0.0000	0.0000	0.0000
8.04	1.0826	0.9619	0.8881	0.9775	0.0000	0.0000	0.0000	0.0000
10.42	1.4609	1.4899	0.9012	1.2840	0.0000	0.0000	0.0000	0.0000
14.42	0.9288	0.6666	1.1524	0.9159	0.0000	0.0000	0.0000	0.0000
20.42	1.4745	1.2059	1.2783	1.3196	0.0000	0.0000	0.0000	0.0000

Time (d)	A + error	A - error	B + error	B - error	C + error	C - error	D + error	D - error
0.02	0.0000	0.0000	0.0000	0.0000	0.0000	0.0000	0.0000	0.0000
1.04	0.0915	0.1562	0.0774	0.1399	0.0468	0.0698	0.0000	0.0000
2.17	0.1468	0.1142	0.3460	0.3228	0.1677	0.1754	0.0000	0.0000
2.94	0.1728	0.1646	0.2183	0.2504	0.1519	0.0897	0.0000	0.0000
4.04	0.1851	0.1512	0.2552	0.1768	0.1058	0.1628	0.0000	0.0000
6.04	0.1487	0.2367	0.1804	0.1139	0.2353	0.1472	0.0000	0.0000
8.04	0.0625	0.0709	0.3355	0.2755	0.1051	0.0895	0.0000	0.0000
10.42	0.1513	0.1073	0.0873	0.1165	0.2059	0.3828	0.0000	0.0000
14.42	0.3404	0.3666	0.3820	0.3060	0.2365	0.2493	0.0000	0.0000
20.42	0.2069	0.2007	0.2622	0.2570	0.1549	0.1137	0.0000	0.0000

Notes:
1. All samples were filtered through a 0.2 micron membrane, preserved with 2 N HCl, and analyzed by GFAA.
2. Filtered/ultracentrifuged samples were spun at 109,000 rcf for 1 h.
3. Data were normalized by subtracting the concentration of arsenic present in the first sample taken immediately after inoculation.
4. +/- errors were determined by calculating the difference between either the maximum or minimum value and the average value at each sampling time.

Appendix P

Title: Fraction of total iron or arsenic that passed through the 0.2 micron membrane.

Data presented in Figure 15

Key:
A = Abiotic trials with 100uM loaded As (3 replicates)
B = Biotic trials with 50uM loaded As (3 replicates)
C = Biotic trials with 100uM loaded As (3 replicates)
D = Biotic trials with no As (3 replicates)

Fraction of total Fe that passed through the filter

Time (days)	A avg	B avg	C avg	D avg
0.02	0.0000	0.0000	0.0000	0.0000
1.04	0.0001	-0.0012	0.0050	0.0031
2.17	0.0003	0.0128	0.0206	0.0162
2.94	0.0035	0.0249	0.0309	0.0267
4.04	0.0053	0.0539	0.0760	0.0488
6.04	0.0083	0.0950	0.1342	0.1018
8.04	0.0116	0.2046	0.1904	0.2006
10.42	0.0084	0.2537	0.3642	0.2318
14.42	0.0150	0.4288	0.5330	0.4393
20.42	0.0036	0.5601	0.7074	0.5765

Fraction of total As that passed through the filter

Time (days)	A avg	B avg	C avg
0.02	0.0000	0.0000	0.0000
1.04	-0.0002	0.0027	0.0041
2.17	-0.0002	0.0052	0.0111
2.94	0.0001	0.0119	0.0182
4.04	0.0005	0.0202	0.0345
6.04	0.0026	0.0613	0.0897
8.04	0.0030	0.1492	0.1309
10.42	0.0057	0.2268	0.2607
14.42	0.0100	0.4595	0.5058
20.42	0.0123	0.8853	0.7334

Notes:
1. Samples were filtered through a 0.2 micron membrane and preserved with 2 N HCl.
2. Samples analyzed for total iron (Fe(II) + Fe(III)) were digested in 0.5 N HCl.
3. The fraction of total iron was calculated by dividing the concentration of total iron that passed through the filter by the total iron present in the microcosm, 59.1mM Fe.

4. The fraction of total arsenic was calculated by dividing the concentration of arsenic that passed through the filter by the total arsenic loaded on the iron gel initially; 100uM As for trials A and C, and 50uM As for trial B.
5. Data from the filtered and filtered/ultracentrifuged samples were normalized by subtracting the concentration of total iron present or arsenic in the first sample taken immediately after inoculation.